

LOW-FLOW TRAVELTIME, LONGITUDINAL-DISPERSION, AND REAERATION  
CHARACTERISTICS OF THE SOURIS RIVER FROM LAKE DARLING DAM TO  
J. CLARK SALYER NATIONAL WILDLIFE REFUGE, NORTH DAKOTA

By Edwin A. Wesolowski, U.S. Geological Survey and  
Richard A. Nelson, North Dakota State Department of Health

---

U.S. GEOLOGICAL SURVEY

Water-Resources Investigations Report 87-4241

Prepared in cooperation with the  
NORTH DAKOTA STATE DEPARTMENT OF HEALTH

Bismarck, North Dakota

1987



DEPARTMENT OF THE INTERIOR

DONALD PAUL HODEL, Secretary

U.S. GEOLOGICAL SURVEY

Dallas L. Peck, Director

---

For additional information write to:

District Chief  
U.S. Geological Survey  
821 East Interstate Avenue  
Bismarck, ND 58501

Copies of this report can be  
purchased from:

U.S. Geological Survey  
Books and Open-File Reports  
Federal Center, Bldg. 810  
Box 25425  
Denver, CO 80225

## CONTENTS

	<u>Page</u>
Glossary of terms-----	vii
Abstract-----	1
Introduction-----	1
Objective and scope-----	2
Acknowledgments-----	3
Location and hydrology-----	3
Study-reach description-----	5
Subreach descriptions-----	5
Test-reach selection and description-----	13
Determination of low-flow traveltime, longitudinal-dispersion, and reaeration characteristics-----	15
Tracer technique and data collection-----	16
Traveltime and longitudinal-dispersion results-----	19
Adjustment to measured dye concentrations-----	23
Uses of dispersion data-----	32
Reaeration results-----	32
Experimental values-----	34
Predictive-equation values-----	35
Summary-----	40
Selected references-----	42
Supplement 1. Perspective plots of cross sections-----	45
2. Measured dye concentrations as a function of traveltime-----	53
3. Traveltime as a function of distance relations-----	57
4. Reconstruction and calculation of area under concentration-time curve for the Logan test reach using total-recovery equation-----	61
5. Measured-, conservative-, and unit-peak dye concentrations as a function of traveltime-----	62

## ILLUSTRATIONS

Figure 1. Map showing Souris River basin, United States and Canada-----	4
2. Map showing location of subreaches and test reaches within the study reach-----	6
3-9. Photographs of:	
3. Farmer-built dam and equipment crossing in the Foxholm subreach-----	9
4. Pooled section of the Souris River in the Logan subreach-----	9
5. Riffle section of the Souris River in the Logan subreach-----	10
6. Typical section of the Souris River in the Velva subreach-----	10
7. Scattered trees in channel in the Velva subreach-----	11
8. Large tree jam in the Velva subreach-----	11
9. Typical tree jam in the Velva subreach-----	12

ILLUSTRATIONS, Continued

	<u>Page</u>
Figure 10. Photograph of pooled section of the Souris River in the Towner subreach-----	12
11. Diagram showing layout of tracer-injection equipment-----	18
12. Diagram showing definition of the concentration-time curves resulting from dye injection-----	20
13. Graph showing attenuation of unit-peak concentrations with traveltime for: Foxholm test reach, September 6-11, 1983; Minot test reach, September 7-10, 1983-----	27
14. Graph showing attenuation of unit-peak concentrations with traveltime for: Logan test reach, September 14-17, 1983; Velva test reach, September 14-16, 1983; and Towner test reach, September 27-29, 1983-----	28
15. Six cross sections in the Foxholm test reach, September 9, 1983-----	45
16. Five cross sections in the Minot test reach, September 21, 1983-----	47
17. Nine cross sections in the Logan test reach, September 22, 1983-----	48
18. Five cross sections in the Velva test reach, September 28, 1983-----	50
19. Seven cross sections in the Towner test reach, September 27, 1983-----	51
20-30. Graphs showing:	
20. Measured dye concentrations as a function of traveltime, Foxholm test reach, September 6-11, 1983-----	53
21. Measured dye concentrations as a function of traveltime, Minot test reach, September 7-10, 1983-----	53
22. Measured dye concentrations as a function of traveltime, Logan test reach, September 14-17, 1983-----	54
23. Measured dye concentrations as a function of traveltime, Velva test reach, September 14-16, 1983-----	55
24. Measured dye concentrations as a function of traveltime, Towner test reach, September 27-29, 1983-----	56
25. Traveltime as a function of distance relations for the Foxholm and Minot test reaches-----	57
26. Traveltime as a function of distance relations for the Logan test reach, September 14-17, 1983-----	58
27. Traveltime as a function of distance relations for the Velva test reach, September 14-16, 1983-----	59
28. Traveltime as a function of distance relations for the Towner test reach, September 27-29, 1983-----	60
29. Measured-, conservative-, and unit-peak dye concen- trations as a function of traveltime for the Foxholm test reach-----	62
30. Measured-, conservative-, and unit-peak dye concen- trations as a function of traveltime for the Minot test reach-----	63

## ILLUSTRATIONS, Continued

Page

Figures 31-33. Graphs showing:

31.	Measured-, conservative-, and unit-peak dye concentrations as a function of traveltime for the Logan test reach-----	64
32.	Measured-, conservative-, and unit-peak dye concentrations as a function of traveltime for the Velva test reach-----	65
33.	Measured-, conservative-, and unit-peak dye concentrations as a function of traveltime for the Towner test reach-----	66

### TABLES

Table	1. Description of subreaches-----	7
	2. Description of test reaches-----	14
	3. Data collected during traveltime measurements-----	22
	4. Conservative-peak and unit-peak dye concentrations-----	26
	5. Area, centroid, and variance of concentration-time data computed by computer program and longitudinal-dispersion coefficients and mixing times for selected test reaches, September 1983-----	31
	6. Peak concentrations and traveltime of peak concentrations for ethylene and propane tracer gases and rhodamine-WT dye, September 1983-----	34
	7. Reaeration coefficients ( $K_2$ ) for ethylene and propane determined using peak computation methods, September 1983-----	35
	8. Comparison of reaeration coefficients determined using measured data (September 1983) with those determined using velocity-depth (empirical) equations-----	36
	9. Comparison of reaeration coefficients determined using measured data (September 1983) with those determined using energy-dissipation (semiempirical) equations-----	37
	10. Geometry of test reaches and traveltime and velocity data collected in the test reaches during September 1983----	38
	11. Error analysis of reaeration coefficients-----	39

## CONVERSION FACTORS

For those readers who may prefer to use metric (International System) units rather than inch-pound units, the conversion factors for inch-pound units used in this report are listed below.

Multiply inch-pound unit	By	To obtain metric unit
Acre-foot (acre-ft)	1,233	cubic meter
	0.001233	cubic hectometer
Cubic foot per second (ft <sup>3</sup> /s)	0.02832	cubic meter per second
Cubic foot per second per pound [(ft <sup>3</sup> /s)/lb]	0.0624	cubic meter per second per kilogram
Foot (ft)	0.3048	meter
Foot per foot (ft/ft)	1.0	meter per meter
Foot per mile (ft/mi)	0.1894	meter per kilometer
Foot per second (ft/s)	0.3048	meter per second
Foot per second per second [(ft/s)/s]	0.3048	meter per second per second
Inch (in.)	25.4	millimeter
Mile (mi)	1.609	kilometer
Pound (lb)	0.4536	kilogram
Square foot per second (ft <sup>2</sup> /s)	0.0929	square meter per second
Square mile (mi <sup>2</sup> )	2.59	square kilometer
Yard (yd)	0.9144	meter

Degree Celsius (°C) may be converted to degree Fahrenheit (°F) as follows:  

$$^{\circ}\text{F} = 9/5^{\circ}\text{C} + 32$$

## GLOSSARY OF TERMS

- $A_c$ , mean area under the total concentration-time curve, in micrograms per liter-hour, that represents the dye-cloud mass.
- $C_{con}$ , conservative dye concentration (solute), in micrograms per liter.
- $C_{d_1}$ ,  $C_{d_2}$ , peak concentration of dye at the upstream and downstream sampling cross sections, respectively, in micrograms per liter.
- $C_{g_1}$ ,  $C_{g_2}$ , peak concentration of the tracer gas at the upstream and downstream sampling cross sections, respectively, in micrograms per liter.
- $C_{meas}$ , measured dye concentration, in micrograms per liter.
- $C_p$ , peak dye concentration (solute), in micrograms per liter.
- $C_{p_1}$ ,  $C_{p_2}$ , peak dye concentration at sampling sites 1 and 2, in micrograms per liter.
- $C_s$ , dye concentration, in micrograms per liter.
- $C_u$ , unit dye concentration (solute), in micrograms per liter times cubic feet per second per pound.
- $c_1$ ,  $c_2$ , centroid of the dye cloud at sampling sites 1 and 2.
- $^{\circ}C$ , degrees Celsius.
- $d$ , day.
- $F$ , Froude number.
- $g$ , acceleration due to gravity, 32.2 [(ft/s)/s].
- $H$ , hydraulic depth, in feet.
- $\bar{H}$ , mean hydraulic depth, in feet.
- $h$ , hour
- $J_2$ , dye-loss correction factor between the upstream and downstream sampling cross sections.
- $K_g$ , desorption coefficient for the tracer gas, base e logarithm, per day.
- $K_x$ , longitudinal-dispersion coefficient, in square feet per second.
- $K_2$ , reaeration coefficient, base e logarithm, per day.

$K_2 \text{ exp}$ , reaeration coefficient measured experimentally.

$K_2 \text{ pred}$ , reaeration coefficient predicted by equations.

$L$ , distance from the point of maximum surface velocity to the farthest bank, approximately one-half the stream width, in feet.

$\ln$ , natural logarithm, base  $e$ .

min, minute.

mL, milliliter

$\mu\text{g/L}$ , micrograms per liter. Micrograms per liter is a unit expressing the concentration of a chemical constituent in solution as weight (micrograms) of solute per unit volume (liter) of water.

$\mu\text{g-h/L}$ , micrograms-hour per liter.

$PE$ , error of estimate.

$Q$ , discharge at the point of sampling, in cubic feet per second.

$R$ , ratio of the absorption coefficient for oxygen to the desorption coefficient for the tracer gas (determined in the laboratory).

$R_p$ , percentage of dye recovered, percent.

$S$ , slope of the energy gradient, in foot per foot.

Sea level, in this report sea level refers to the National Geodetic Vertical Datum of 1929 (NGVD of 1929)--a geodetic datum derived from a general adjustment of the first-order level nets of both the United States and Canada, formerly called mean sea level of 1929.

$\sigma^2 t_1$ , variance of the concentration-time curve at the upstream sampling cross section, in hours squared.

$\sigma^2 t_2$ , variance of the concentration-time curve at the downstream sampling cross section, in hours squared.

$t$ , mean test-reach water temperature, in degrees Celsius.

$t_c$ , mean traveltime of centroid from sampling site 1 to sampling site 2.

$T_{c1}$ ,  $T_{c2}$ , cumulative traveltime since injection and arrival of centroid at sampling sites 1 and 2.

$t_{d1}$ , time necessary for entire dye cloud to pass sampling site 1.

$T_e$ , cumulative traveltime of the arrival of the leading edge of the dye cloud.

$T_{e1}$ , cumulative traveltime since injection and arrival of leading edge of the dye cloud at sampling site 1.

$T_{f1}$ , cumulative traveltime since injection and arrival of trailing edge of the dye cloud at sampling site 1.

$t_p$ , mean traveltime of peak concentration of the dye cloud from sampling site 1 to sampling site 2.

$T_{p1}$ ,  $T_{p2}$ , cumulative traveltime since injection and arrival of peak concentration of the dye cloud at sampling sites 1 and 2.

$\bar{t}_1$ ,  $\bar{t}_2$ , mean time of passage of the tracer cloud (centroid) past each sampling cross section, in hours.

$t_1$ ,  $t_2$ , traveltime of the peak concentrations of dye at the upstream and downstream sampling cross sections, respectively, in hours.

$U$ , mean velocity, in foot per second.

$\bar{U}$ , mean peak velocity, in feet per second.

$U^*$ , shear velocity, in feet per second.

$V$ , volt.

$Vol$ , volume of 5-percent dye injected, in liters.

$W_d$ , weight of pure dye injected, in pounds.

LOW-FLOW TRAVELTIME, LONGITUDINAL-DISPERSION, AND REAERATION  
CHARACTERISTICS OF THE SOURIS RIVER FROM LAKE DARLING DAM TO  
J. CLARK SALYER NATIONAL WILDLIFE REFUGE, NORTH DAKOTA

By Edwin A. Wesolowski, U.S. Geological Survey, and  
Richard A. Nelson, North Dakota State Department of Health

ABSTRACT

*As part of the Souris River water-quality assessment, traveltime, longitudinal-dispersion, and reaeration measurements were made during September 1983 on segments of the 186-mile reach of the Souris River from Lake Darling Dam to the J. Clark Salyer National Wildlife Refuge. The primary objective was to determine traveltime, longitudinal-dispersion, and reaeration coefficients during low flow. Streamflow in the reach ranged from 10.5 to 47.0 cubic feet per second during the measurement period.*

*On the basis of channel and hydraulic characteristics, the 186-mile reach was subdivided into five subreaches that ranged from 18 to 55 river miles in length. Within each subreach, representative test reaches that ranged from 5.0 to 9.1 river miles in length were selected for tracer injection and sample collection. Standard fluorometric techniques were used to measure traveltime and longitudinal dispersion, and a modified tracer technique that used ethylene and propane gas was used to measure reaeration. Mean test-reach velocities ranged from 0.05 to 0.30 foot per second, longitudinal-dispersion coefficients ranged from 4.2 to 61 square feet per second, and reaeration coefficients based on propane ranged from 0.39 to 1.66 per day.*

*Predictive reaeration coefficients obtained from 18 equations (8 semiempirical and 10 empirical) were compared with each measured reaeration coefficient by use of an error-of-estimate analysis. The predictive reaeration coefficients ranged from 0.0008 to 3.4 per day. A semiempirical equation that produced coefficients most similar to the measured coefficients had the smallest absolute error of estimate (0.35). The smallest absolute error of estimate for the empirical equations was 0.41.*

INTRODUCTION

In 1977 the State of North Dakota adopted stream water-quality standards "\*\*\* to maintain and improve the quality of waters in the State and to maintain and protect existing water uses." (North Dakota State Department of Health, 1977, p. 1). Specific standards, which are based on beneficial uses and on the quality of water existing in 1967, were established for designated classes of waters for the State. The Souris River is designated as a class IA stream. A class IA designation prescribes water-quality standards to ensure the present and future quality

of the Souris River for the following beneficial uses: (1) Agricultural; (2) domestic and municipal; (3) industrial; and (4) recreation, fishing, and wildlife.

The North Dakota State Department of Health (1979) made an appraisal of the Souris River water quality during 1976-78 for the North Dakota Statewide 208 Water Quality Management Plan. Their appraisal indicated some degradation had occurred along some reaches since 1967. To determine the causes for the water-quality degradation, the U.S. Geological Survey, in cooperation with the North Dakota State Department of Health, conducted a water-quality assessment of the Souris River during 1982 and 1983.

### Objective and Scope

The objectives of the Souris River water-quality assessment are to: (1) Define the hydrologic system and the current water-quality problems; (2) determine low-flow traveltime, longitudinal-dispersion, and reaeration characteristics; (3) quantitatively evaluate the water-quality process; and (4) develop conceptual and mathematical models to evaluate the waste-assimilation and water-quality relations. This report (hereafter referred to as the tracer study) addresses objective 2 of the Souris River water-quality assessment; namely, to determine the low-flow traveltime, longitudinal-dispersion, and reaeration characteristics. These characteristics could be used as data in a mathematical model that estimates the waste-assimilation capacity of the river.

The study reach consists of the part of the Souris River from Lake Darling Dam to J. Clark Salyer National Wildlife Refuge. During low flow the study reach is 186 river mi in length. During higher flows the study reach is less than 186 river mi because the river channel in the vicinity of Minot, N. Dak., has been rechanneled; this eliminates some meanders in order to convey flood flows more expeditiously. The study reach was divided into five subreaches that ranged from 18 to 55 river mi in length and were designated: Foxholm, Minot, Logan, Velva, and Towner. Within each subreach, a representative test reach was selected for the tracer studies. These representative test reaches ranged from 5.0 to 9.1 river mi in length.

Dye- and gas-tracing techniques were used to determine low-flow traveltime, longitudinal-dispersion, and reaeration characteristics in the representative reaches. The tracer study was conducted during September 1983 to coincide with low flow in the river under open-water conditions. To accomplish the tracer-study objective and the downstream National Wildlife Refuge management objectives, a flow release from Lake Darling of 10 ft<sup>3</sup>/s was selected. During September, a flow of 10 ft<sup>3</sup>/s can be expected to be exceeded about 60 percent<sup>1</sup> of the time.

<sup>1</sup>Souris River near Foxholm, station 05116000, duration table of daily discharge values (water years 1937-83), U.S. Geological Survey, Bismarck, N. Dak., unpublished data.

Arrangements were made with the U.S. Fish and Wildlife Service to decrease discharge and to maintain a flow of 10 ft<sup>3</sup>/s from Lake Darling for 5 weeks beginning August 22, 1983. During the 5 weeks, the sampling for the tracer study and the synoptic sampling for the waste-assimilation study would be accomplished. The Des Lacs National Wildlife Refuge would not be discharging any water from storage, so only seepage flow, maximum of about 1 to 2 ft<sup>3</sup>/s, was expected from the Des Lacs River. At the same time, the municipalities of Minot, Velva, and Towner were to be draining their waste-stabilization ponds into the Souris River. Drainage from the waste-stabilization ponds was to be at rates that could be sustained for the duration of the tracer study and synoptic sampling. Flows in the downstream part of the study reach (Souris River near Bantry, station 05122000) were expected to range from 20 to 30 ft<sup>3</sup>/s.

#### Acknowledgments

The authors thank the landowners and residents along the Souris River for permitting access to stream sites during periods of data collection for this study. The authors are grateful for the cooperation received from the cities of Minot, Velva, and Towner who maintained releases from their waste-stabilization ponds as requested, and from the U.S. Fish and Wildlife Service who maintained releases from Lake Darling as requested.

#### LOCATION AND HYDROLOGY

The Souris River is an international stream draining parts of the United States and Canada (fig. 1). About 9,320 mi<sup>2</sup> of its total drainage area of 24,800 mi<sup>2</sup> is located in the United States. The river originates in Saskatchewan, Canada, flows in a southeasterly direction, and enters the United States near Sherwood, N. Dak. It continues from Sherwood in a southeasterly direction to a point about 50 mi southeast of Minot, N. Dak. (near Velva), where it changes course, eventually flows northwestward for about 90 mi, and then enters Manitoba, Canada, near Westhope, N. Dak. About 360 mi of the river's total length of 790 mi is located in the United States. Locally, this 360-mi U-shaped part of the river is referred to as the Souris Loop.

The Des Lacs River is the major tributary of the Souris River within the United States. Other tributaries within the United States include the Deep and Wintering Rivers and Boundary and Willow Creeks. Both the Des Lacs and Souris Rivers are impounded and are designated as National Wildlife Refuges for part of their lengths.

Eleven impoundments exist on the Souris River within the refuges. Lake Darling, which is within the Upper Souris National Wildlife Refuge, is the largest impoundment on the Souris River and has a storage capacity of 112,000 acre-ft. Five smaller impoundments located just downstream from Lake Darling have a combined storage capacity of 3,808 acre-ft



(ranging from 144 to 2,884 acre-ft). The remaining five impoundments are located within the J. Clark Salyer National Wildlife Refuge on the Souris River downstream from Bantry. These five impoundments have a combined storage capacity of about 55,100 acre-ft (ranging from about 5,370 to 23,400 acre-ft). Flow in the study reach is controlled by Lake Darling Dam or by the impoundments just downstream from Lake Darling. Operation of Lake Darling Dam began in about 1936 to provide a regulated supply of water to the smaller downstream impoundments and especially to the larger impoundments on the J. Clark Salyer National Wildlife Refuge. Lake Darling Dam has limited flood control.

Annual streamflow in the Souris River varies greatly and depends mostly on the magnitude of spring runoff. For example, the smallest total annual flow to pass the Souris River near Foxholm gage (station 05116000) during water years 1937-83 was 1,210 acre-ft (water year 1937) and the largest total annual flow was 686,300 acre-ft (water year 1976). The median of the mean annual flow for the period of record is 47,500 acre-ft. Total annual flow for water year 1983 was 146,200 acre-ft, which is about three times larger than the median of the mean annual flow.

Monthly flows also are variable. After spring runoff, flow releases from Lake Darling are determined by National Wildlife Refuge management objectives, one of which is to maintain the operational level of the lake (elevation of 1,596 ft) and of the downstream marshes. Monthly mean flows for September at the Souris River near Foxholm gage for water years 1937-83 range from 0 ft<sup>3</sup>/s (water years 1937, 1962, and 1963) to more than 160 ft<sup>3</sup>/s (water year 1955), and the mean monthly flow for September is about 40 ft<sup>3</sup>/s.

#### STUDY-REACH DESCRIPTION

In the study reach, the Souris River drains an area that predominantly produces agricultural products. Deciduous trees, which provide winter shelter for livestock, line the banks of the river and occupy the narrow flood plain. The river flows slowly within its almost flat-sloped meandering channel, which has been modified by human and animal activities. Numerous farmer- or rancher-built dams, which are used as farm equipment and cattle crossings, submerge naturally occurring riffles and deepen pools. Beaver dams, also present in the study reach, have the same effect of submerging riffles and deepening pools.

The physical and hydraulic characteristics of the river change along the 186-river-mi study reach; therefore, based on information obtained from topographic maps and from prior onsite work, the study reach was subdivided into five representative subreaches--Foxholm, Minot, Logan, Velva, and Towner.

#### Subreach Descriptions

The Foxholm subreach (fig. 2) is 18 river mi long and has a slope of about 0.53 ft/mi (table 1). The river channel in the upstream part of the

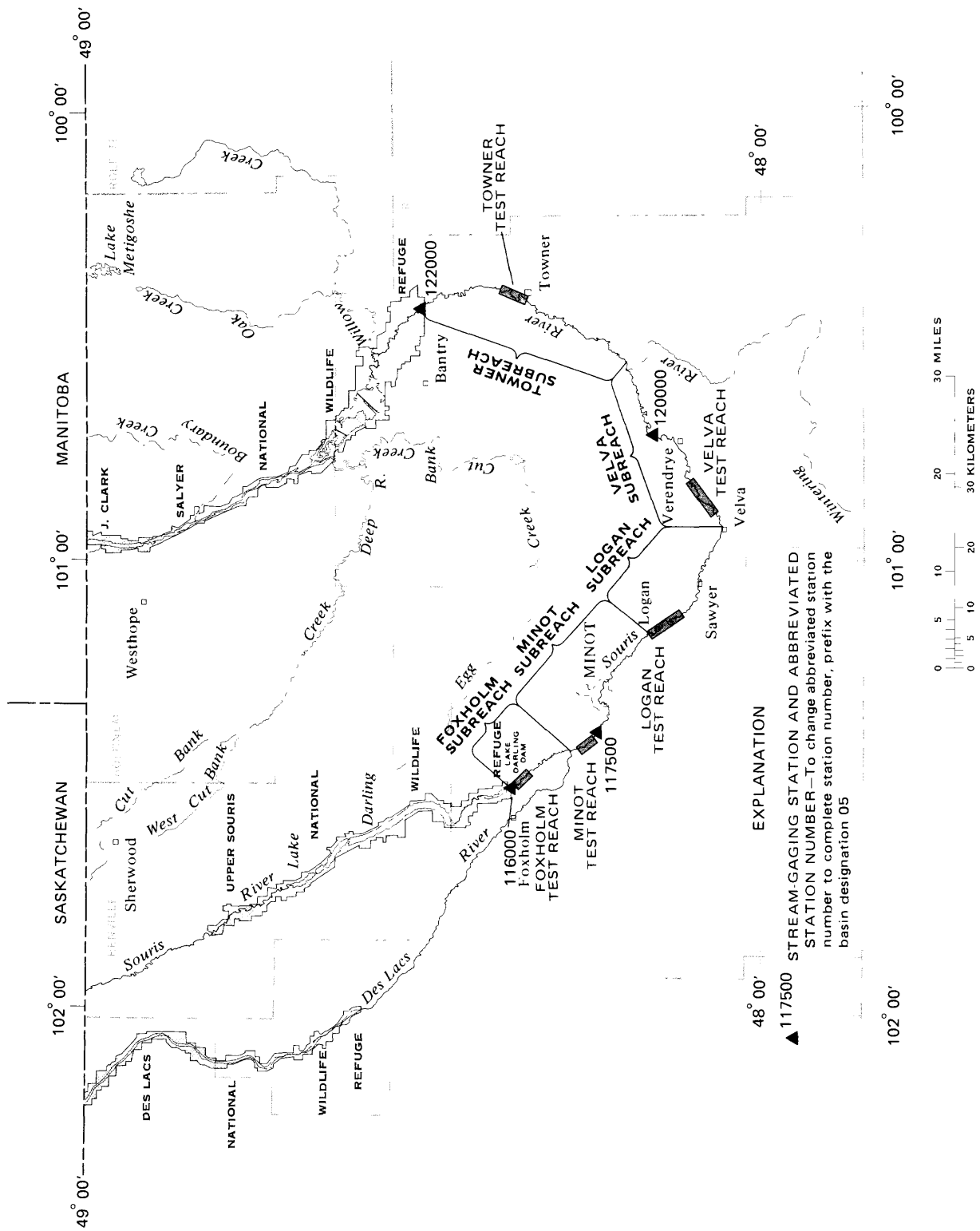


Figure 2.—Location of subreaches and test reaches within the study reach.

Table 1.--Description of subreaches

Subreach name	Beginning and ending river mile	Length (river miles)	Slope (S) (foot per mile) <sup>1</sup>	Slope (S) (foot per foot) <sup>1</sup>	Location
Foxholm	414 - 396	18	0.53	$1.00 \times 10^{-4}$	Souris River near Foxholm stream-gaging station to junction with Des Lacs River.
Minot	396 - 364	32	.92	$1.74 \times 10^{-4}$	Junction of Des Lacs River and Souris River to Souris River near Logan.
Logan	364 - 328	36	.92	$1.74 \times 10^{-4}$	Souris River near Logan to Souris River near Velva.
Velva	328 - 283	45	.76	$1.44 \times 10^{-4}$	Souris River near Velva to junction with Wintering River.
Towner	283 - 228	55	.44	$.83 \times 10^{-4}$	Junction of Wintering River and Souris River to Souris River near Bantry stream-gaging station.

<sup>1</sup>Calculated from decrease in elevation of thalweg, water-surface profile, Souris River, North Dakota (from U.S. Army Corps of Engineers, St. Paul District, written commun., 1970).

subreach has dense, rooted vegetation that extends from the shore toward the middle of the channel and decreases the effective area of flow. Numerous farmer- or rancher-built dams exist throughout this subreach. A typical example is shown in figure 3. U.S. Geological Survey stream-gaging station Souris River near Foxholm (station 05116000) is located at river mi 413.8.

The Minot subreach is 32 river mi long and has a slope of about 0.92 ft/mi. It is similar to the Foxholm subreach with respect to channel vegetation and backwater but, in addition, it has occasional tree jams that block the channel. The part of the subreach that passes through the city of Minot has been cleared of tree jams and has been rechanneled to permit high flows to bypass some of the river meanders. During low flows, gabion-type dams direct the flow to follow the natural channel. U.S. Geological Survey stream-gaging station Souris River above Minot (station 05117500) is located at river mi 388.5.

The Logan subreach is 36 river mi long and has a slope of 0.92 ft/mi. This subreach is a transitional subreach. The river channel in the upstream part of the subreach is wider, deeper, and contains backwater (fig. 4) similar to the Foxholm and Minot subreaches, but the channel in the downstream part is narrower, shallower, and free-flowing (fig. 5) and is similar to the channel in the Velva subreach. The downstream part of the Logan subreach has exposed gravel and rock riffles that do not create pools as deep as those created by the farmer- or rancher-built dams in the upstream Foxholm and Minot subreaches; also, there isn't as much backwater. More tree jams occur in this subreach than in the two upstream subreaches. The upstream part of the Logan subreach receives effluent from Minot's waste-stabilization pond.

The Velva subreach is 45 river mi long and has a slope of 0.76 ft/mi. The river channel in the Velva subreach is the narrowest and shallowest of the five subreaches (fig. 6 shows a typical section of the river) and also has numerous exposed gravel and rock riffles. Tree jams are more numerous and are larger than tree jams in other subreaches. These tree jams vary in size from a few scattered trees in the river channel (fig. 7) to many trees piled on top of each other (fig. 8). The larger tree jams fill the river channel from bank to bank and may be as much as 6 ft high and 40 ft long. A typical tree jam is shown in figure 9. The upstream part of the subreach receives effluent from Velva's waste-stabilization pond. U.S. Geological Survey stream-gaging station Souris River near Verendrye (station 05120000) is located at river mi 302.0.

The Towner subreach is 55 river mi long and has a slope of 0.44 ft/mi. In the middle of this subreach, the river channel becomes deeper and wider and contains backwater (fig. 10). The downstream part of the subreach receives effluent from Towner's waste-stabilization pond just upstream from the city of Towner. U.S. Geological Survey stream-gaging station Souris River near Bantry (station 05122000) is located at river mi 228.0.



**Figure 3.—Farmer-built dam and equipment crossing in the Foxholm subreach. This was the second sampling cross section in the Foxholm test reach and is located at river mile 411.3. Discharge is 14 cubic feet per second. Mean depth is 0.3 foot, maximum depth is about 0.8 foot, and width is 104 feet in cross section (9-9-83).**



**Figure 4.—Pooled section of the Souris River in the Logan subreach. This is where a cross section of the channel was made and is located at about river mile 363.6 (looking downstream). Discharge is about 14 cubic feet per second. Mean depth is 2 feet, maximum depth is 3.5 feet, and width is 67 feet (9-22-83).**



**Figure 5.—Riffle section of Souris River in the Logan subreach. This is the first sampling cross section in the Logan test reach at about river mile 362.6 (looking upstream). Discharge is about 14 cubic feet per second (9-22-83).**



**Figure 6.—Typical section of the Souris River in the Velva subreach. This is the second sampling cross section in the Velva test reach at about river mile 318.9. Discharge is 26 cubic feet per second. Mean depth is 1.2 feet, maximum depth is 1.8 feet, and width is 30 feet in cross section (9-28-83).**



**Figure 7.**—Scattered trees in channel in the Velva subreach. This is the injection site at river mile 323.1 (looking downstream). Discharge is about 43 cubic feet per second (9-21-82).



**Figure 8.**—Large tree jam in the Velva subreach. Tree jam is just upstream from the second sampling cross section in the Velva test reach at river mile 320.7 (looking downstream). Discharge is 45.5 cubic feet per second. Mean depth of three cross sections is 2.3 feet, maximum depth is 4.1 feet, and mean width of three cross sections is 49 feet (9-21-82).



**Figure 9.**—Typical tree jam in the Velva subreach. Tree jam is at about river mile 319. Discharge is 26 cubic feet per second (9-28-83).



**Figure 10.**—Pooled section of the Souris River in the Towner subreach. This is where a cross section of the channel was made and is located at about river mile 250.8 (looking downstream). Discharge is 46 cubic feet per second. Mean depth is 4.0 feet, maximum depth is 5.7 feet, and width is 64 feet (9-27-83).

## Test-Reach Selection and Description

Once the subreaches were defined, it was necessary to locate a representative test reach within each subreach that would be suitable for tracer injection and subsequent sample collection. During September 1982, a reconnaissance trip was made to: (1) Locate a test reach within each subreach; (2) select one of the test reaches for an equipment test; and (3) provide practical experience for the three, two-member crews involved in the study. A canoe trip was made through parts of each test reach to obtain data from selected cross sections in order to estimate mean width, depth, and velocity. Some of the criteria for test-reach selection were to: (1) Locate sites representative of the subreach; (2) locate vehicle and equipment access to the site; and (3) locate at least one cross section that would be suitable for making a low-flow discharge measurement. The test reaches were named the same as the subreaches: Foxholm, Minot, Logan, Velva, and Towner.

The Velva test reach was selected for the equipment test. Tracer injection was made September 21, 1982, and tracer samples were collected at six downstream sites (0.2, 1.1, 2.4, 5.1, 7.9, and 12.6 river mi from the injection site). Some of the findings and conclusions of the test were: (1) The dye was not uniformly mixed at the 0.2-river-mi site--the distance and traveltime between the injection site and the first sampling site must be increased to about a mile, or 2-3 h traveltime; (2) the dye cloud arrived much earlier than expected, and the peak was missed at the 5.1-river-mi site because of inaccurate mean-velocity estimates--remove consequence of error in velocity estimates and subsequent arrival of leading edge of the dye cloud by having sampling team onsite several hours before dye cloud is expected; and (3) gas concentration was less than 1  $\mu\text{g/L}$  in the samples collected at the 7.9-river-mi site, and almost no gas was detected in samples collected from the 12.6-river-mi site (about 60 h traveltime)--shorten test-reach lengths so that gas peak arrives at the most downstream sampling cross section in shorter traveltime.

One of the few mechanical problems discovered during the equipment test was the freezing of the regulating valve on the ethylene cylinder during injection. The freezing occurred only when a full gas cylinder was used for the first time. Therefore, 2 to 3 lb of ethylene was degassed from new cylinders before use. Another problem was the inability to communicate with members of the sampling teams over long distances using citizen-band radios. Mobile or portable radios were acquired from surplus equipment, repaired, and installed in each vehicle that would be involved in the tracer study.

During September 1983, a second canoe trip was made through each test reach either during or after the study to measure stream widths, depths, and discharges. Stream widths were measured at the beginning and end of each test reach and at every river-mile point in-between. Cross sections were measured by taking soundings at either 2- or 5-ft intervals at each cross section. Descriptions of test reaches are summarized in table 2. The test reaches ranged in length from 5.0 to 9.1 river mi. The range of mean hydraulic depth (total cross-sectional areas divided by total cross-sectional widths) for the test reaches was 1.4 to 3.4 ft, and the range of

Table 2.--Description of test reaches

Test reach	Beginning and ending river mile	Length (river miles)	Date	Number of cross sections	Depth		Width		Measured stream discharge (cubic feet per second)
					Mean hydraulic (feet)	Maximum range (feet)	Mean (feet)	Maximum range (feet)	
Foxholm	413.8-408.8	5.0	09-09-83	6	2.9	2.0-5.9	60	44-86	14
Minot	390.5-385.5	5.0	09-21-83	5	3.4	2.3-8.4	61	52-78	121
Logan	363.9-354.8	9.1	09-22-83	9	2.4	1.5-5.2	52	38-67	226
Velva	322.9-314.1	8.8	09-28-83	5	1.4	1.8-2.6	40	30-48	26
Towner	256.8-250.3	6.5	09-27-83	7	2.6	1.4-5.8	68	41-90	46

<sup>1</sup>Daily mean, Souris River above Minot, N. Dak., stream-gaging station 05117500.

<sup>2</sup>Estimated; based on daily mean, Souris River above Minot, N. Dak., stream-gaging station 05117500, and Souris River near Verendry, N. Dak., stream-gaging station 05120000.

maximum depth was 1.4 to 8.4 ft. The range of mean stream width for the test reaches was 40 to 68 ft and the range of maximum width was 30 to 90 ft. Data for cross-sectional widths and depths were entered into a computer program for analysis of the test-reach channel geometry and for plotting cross sections. The geometry analysis could be used in a mathematical model that estimates the waste-assimilation capacity of the river. Only the perspective plots of the cross sections within each test reach are presented here (supplement 1).

The perspective plots are looking downstream and show all the cross sections within the test reach beginning at the upstream end, which usually was the tracer-injection cross section, and ending with the most downstream sampling cross section. Each cross section shows the shape of the channel at that cross section and the water surface at the time the cross section was measured.

#### DETERMINATION OF LOW-FLOW TRAVELTIME, LONGITUDINAL-DISPERSION, AND REAERATION CHARACTERISTICS

Traveltime and longitudinal-dispersion characteristics of a stream vary with the magnitude of its flow. Measurements of the rate of movement and dispersion of a substance injected into a stream are necessary to define these characteristics during the flow of interest.

Traveltime simply is the measure of the time required for the movement of water or waterborne materials between two points in the stream. Knowing the traveltime and distance between the two points, mean velocities can be computed. The spread of the waterborne materials represents the degree of longitudinal dispersion occurring between two points in the stream.

Accurate mean subreach velocities could not be obtained during the September 1982 reconnaissance because of the variable physical and hydraulic characteristics of the channel and because of the low-flow conditions in the study reach. Velocities were so slow in some pool areas that they could not be measured with a current meter.

Accurate mean subreach velocities, however, can be calculated from traveltime studies that use dye as a tracer. The modified tracer technique of Rathbun and others (1975) used for the reaeration part of this study includes injection of a dye tracer simultaneously with gas tracers. The same dye tracer data used in reaeration studies was used to measure traveltime and longitudinal-dispersion coefficients (Hubbard and others, 1982). Dye-tracer studies will be discussed later in the report in the section entitled "Traveltime and Longitudinal-Dispersion Results."

Mean subreach velocities and longitudinal-dispersion coefficients are required for a waste-assimilation model, but they also have other practical applications. Velocity data are useful when timing the arrival of releases from Lake Darling at downstream marshes. Traveltime and

dispersion data can be used to determine the transport and fate of accidental or planned waste discharges into the river.

One of the most important types of information for determining the waste-assimilation capacity of a stream is the reaeration coefficient. The reaeration coefficient is a measure of the ability of a stream to absorb oxygen from the atmosphere. The more oxygen a stream can absorb, the more oxygen-depleting waste the stream can assimilate. Numerous empirical and semiempirical equations exist in the literature for calculation of the reaeration coefficient. However, according to Rathbun (1977), these predictive equations can result in a considerable range of values for a specific set of hydraulic conditions. Later in this report in the section titled "Predictive Equation Values," a comparison of reaeration coefficients, measured values versus predictive-equation values, is made that supports Rathbun's (1977) conclusion.

To measure the reaeration coefficient of the Souris River, a tracer technique developed by Tsivoglou and others (1968) and modified by Rathbun and others (1975) was used. The modified method uses low-molecular-weight hydrocarbon gases as tracers. The gas-tracer technique is based on the observation that the ratio ( $R$ ) of the rate coefficient for a gas tracer desorbing from water in a stirred tank ( $K_g$ ) to the rate coefficient for oxygen being absorbed by the same water ( $K_2$ ) is a constant regardless of the mixing conditions within the stirred tank; thus,  $R = K_g/K_2$ .

The basic procedure consists of simultaneously injecting quantities of dye and gas tracers into a stream so that both tracers undergo identical dispersion and dilution. The tracers are sampled at various downstream points, and analyzed for their concentrations. To determine the amount of gas desorbed, the conservative dye tracer is used to adjust the nonconservative gas tracer concentration for dispersion and dilution. A desorption coefficient is calculated by comparing the desorption of the gas tracer against the dye tracer, which is not desorbed. The reaeration coefficient for oxygen is computed from the gas tracer desorption coefficient by means of the laboratory-determined constant. These calculations and conversions are discussed later in the report in the section titled "Reaeration Results."

#### Tracer Technique and Data Collection

Three assumptions are inherent in the modified tracer technique as developed by Rathbun and others (1975): (1) The ratio of the desorption coefficient for the gas tracer to the absorption coefficient for oxygen is independent of mixing conditions, temperature, and presence of pollutants for the range of ambient conditions in streams; (2) the dye tracer is essentially conservative; and (3) the nonconservative gas tracer undergoes the same dispersion and dilution as the conservative dye tracer and is lost from the stream only by desorption through the water surface to the atmosphere.

Data collection for the tracer study was conducted during September 1983 and began with simultaneous injection of a solution of rhodamine-WT

fluorescent dye and ethylene and propane gases. Duplicate and simultaneous tests of ethylene and propane gas were made to compare their respective desorption coefficients. Appropriate dye- and gas-rates and concentrations were estimated for stream discharges using equations presented by Rathbun (1979). Tracers were injected continuously for 30- or 60-min-long periods at differing injection rates so that about the same volume was injected in each of the five test reaches. The layout of the tracer-injection equipment is shown in figure 11.

A solution of 5-percent rhodamine-WT dye was injected at midflow between two sets of gas diffusers. A dye-metering pump was used to transfer the dye from a plastic, graduated cylinder through Tygon<sup>2</sup> tubing to the single injection point. To aid in accounting for the quantity of dye used during injection, the dye was prepackaged in 450-mL volumes.

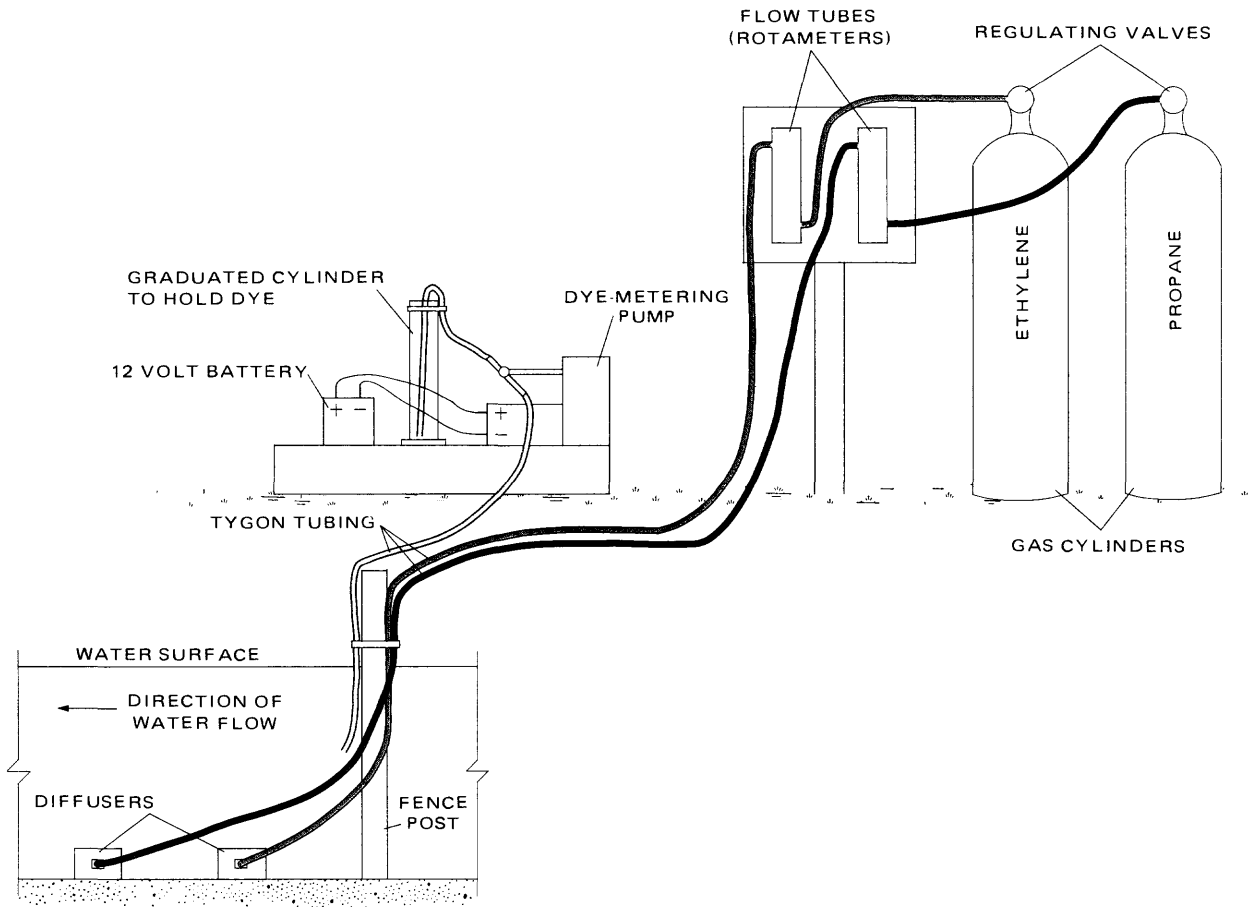
To perform the duplicate tests, ethylene (technical grade) and propane (commercial grade) were injected into the stream by bubbling the gases through four porous, flat, rectangular diffusers (two each for ethylene and propane). The diffusers were placed in the area of the greatest flow either directly on the streambed bottom, or on concrete blocks if the streambed was too soft to support the diffusers. The depth at the injection cross section typically was shallower than the mean subreach depth. Ethylene was released from a high-pressure cylinder, and propane was released from a low-pressure cylinder through two-stage regulating valves (for propane a single-stage valve would have been sufficient) and rotameters that monitored the gas flow to the diffusers. The tracer gases were conveyed through the whole system from the gas cylinders to the diffusers by Tygon tubing.

The movements of the resultant tracer clouds were monitored in at least two sampling cross sections in all test reaches. Dye- and gas-tracer samples were collected simultaneously in the sampling cross sections at midflow. Samples for dye analysis were collected in two 32-mL glass vials strapped to the outside of the gas sampler by a heavy-duty rubber band. Dye samples also were collected periodically at two quarter points in the sampling cross section to determine or verify uniformity of dye concentration by comparing the concentration of the quarter-point samples with the concentration of the midflow sample.

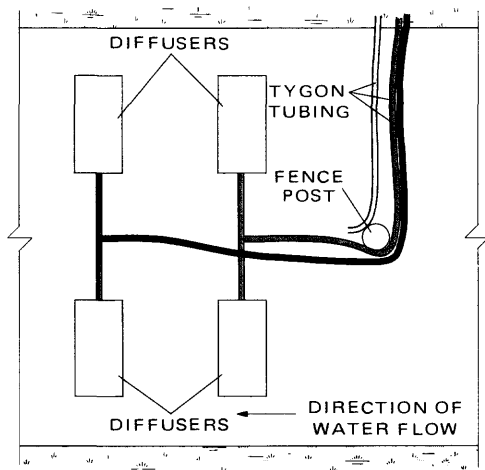
Nonaerated samples for gas analysis were collected in a small-sized, displacement-type sampler containing a glass, 40-mL septum vial. No gas samples were collected at the quarter points.

Dye sampling began before the arrival of the leading edge of the dye cloud to ascertain if any background fluorescence existed. Sampling continued during passage of the dye cloud until sufficient samples were collected to define the complete concentration-time curves and concluded

<sup>2</sup>Use of trade names in this report is for identification purposes only and does not constitute endorsement by the U.S. Geological Survey.



SIDE VIEW



TOP VIEW

Figure 11.—Diagram of tracer-injection equipment (not to scale).

when concentrations decreased to less than 10 percent of the peak dye concentration. Contents of one of the two vials containing samples for dye-concentration analysis were analyzed immediately, and the results recorded. Dye concentrations were analyzed using a fluorometer powered by a 12-V, wet-cell battery and standard fluorometric techniques as described by Wilson and others (1984). Contents of the second vial were stored for later analysis in the U.S. Geological Survey laboratory in Bismarck, N. Dak., where the same recalibrated fluorometer was used to measure all of the dye samples.

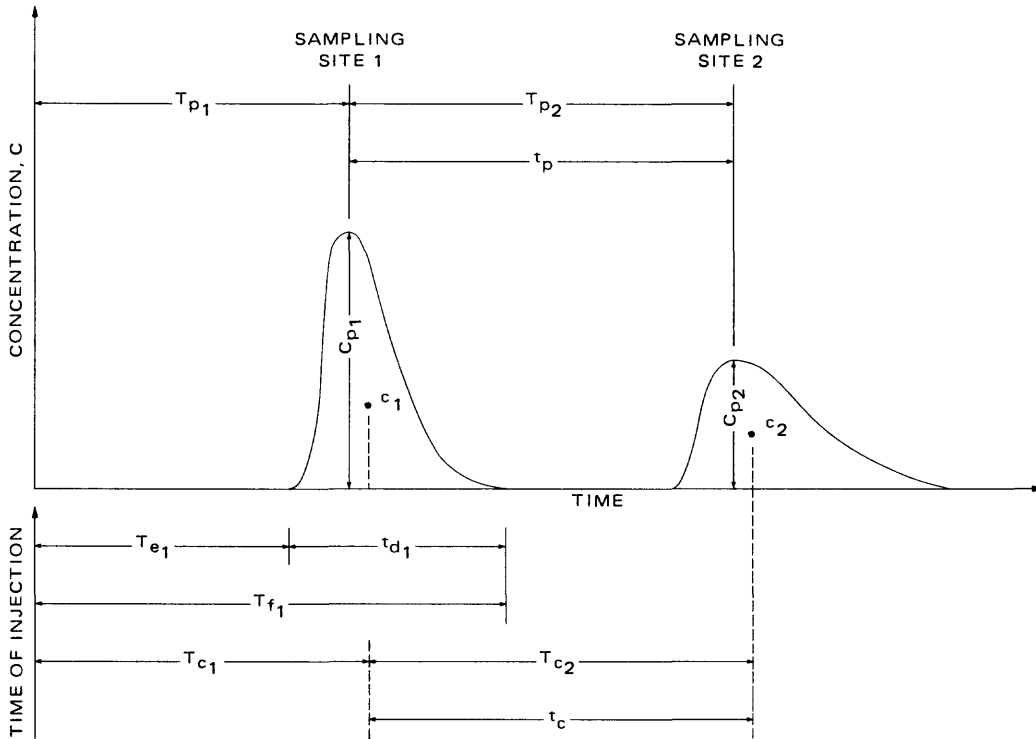
For the gas analysis, a sufficient number of samples were collected to define the peak only. Gas samples were preserved by adding 1 mL of 40-percent formalin to each sample. The gas samples were stored for later analysis at the U.S. Geological Survey laboratory in Atlanta, Ga. Ethylene and propane concentrations in the water samples were determined using a modification of the gas-chromatographic technique of Swinnerton and Linnenbom (1967).

### Traveltime and Longitudinal-Dispersion Results

In each of the five test reaches, measurements were made of the movement, concentration, and dispersion of the dye cloud as it traveled downstream. The dye, when injected into a stream, mixes completely with the water and moves in the same manner as the water molecules. As the dye cloud travels downstream it disperses, taking longer and longer to pass each successive site, and the peak concentration gradually decreases. The dispersion of the dye cloud occurs in all three dimensions of the channel. Vertical dispersion usually is completed first. Complete lateral dispersion occurs somewhat later, depending on the width and velocity variations of the stream. However, uniform dye concentrations in a cross section of a stream may take a long time to occur because dye-tracer particles at the center of the stream travel faster than those near the edge. Finally, longitudinal dispersion has no boundaries and continues indefinitely (Hubbard and others, 1982). Longitudinal dispersion is the dispersion component of primary interest in this study.

Concentration-time curves are the basis for the interpretation of traveltime and longitudinal dispersion. The shapes of these curves are indicators of the traveltime and velocity characteristics of the channel. Concentration-time curves were prepared for each sampling cross section by plotting the measured dye concentration against the time since injection (supplement 2). A smooth curve was drawn through the plotted points. Where necessary, because of missing data, the curves were extrapolated from the concentration of the first sample collected at the leading edge (last sample collected in the instance of the trailing edge) to zero because the total area of the concentration-time curve is required when dye recovery is calculated.

The main features of the curves (fig. 12) are the leading edge, peak, and trailing edge. The centroid, which is a point that represents the center of the area under the concentration-time curve, also is shown in figure 12. These features are described in terms of cumulative traveltime



- $T_{p1}, T_{p2}$  CUMULATIVE TRAVELTIME SINCE INJECTION AND ARRIVAL OF PEAK CONCENTRATION AT SAMPLING SITES 1 AND 2
- $t_p$  MEAN TRAVELTIME OF PEAK CONCENTRATION FROM SAMPLING SITE 1 TO SAMPLING SITE 2
- $C_{p1}, C_{p2}$  PEAK DYE CONCENTRATION AT SAMPLING SITES 1 AND 2
- $c_1, c_2$  CENTROID OF THE DYE CLOUD AT SAMPLING SITES 1 AND 2
- $T_{e1}$  CUMULATIVE TRAVELTIME SINCE INJECTION AND ARRIVAL OF LEADING EDGE AT SAMPLING SITE 1
- $t_{d1}$  TIME NECESSARY FOR ENTIRE DYE CLOUD TO PASS SAMPLING SITE 1
- $T_{f1}$  CUMULATIVE TRAVELTIME SINCE INJECTION AND ARRIVAL OF TRAILING EDGE AT SAMPLING SITE 1
- $T_{c1}, T_{c2}$  CUMULATIVE TRAVELTIME SINCE INJECTION AND ARRIVAL OF CENTROID AT SAMPLING SITES 1 AND 2
- $t_c$  MEAN TRAVELTIME OF CENTROID FROM SAMPLING SITE 1 TO SAMPLING SITE 2

**Figure 12.—Definition of the concentration-time curves resulting from dye injection. (Modified from Hubbard and others, 1982).**

after dye injection. The cumulative traveltime of the arrival of the peak concentration of the dye cloud at sampling sites 1 ( $T_{p1}$ ) and 2 ( $T_{p2}$ ) is shown in figure 12. The calculation of the mean traveltime of the peak concentration of the dye cloud between sampling sites 1 and 2 is:  $t_p = T_{p2} - T_{p1}$ . The calculation of the mean traveltime of the centroid of the dye cloud,  $t_c$ , is similar to the calculation of mean traveltime of the peak concentration of the dye cloud,  $t_p$ , except centroid cumulative traveltimes are used:  $t_c = T_{c2} - T_{c1}$ . The cumulative traveltime of the arrival of the leading edge ( $T_{e1}$ ) and trailing edge ( $T_{f1}$ ) at sampling site 1 also is shown in figure 12. The calculation of the time necessary for the entire dye cloud to pass sampling site 1 is:  $t_{d1} = T_{f1} - T_{e1}$ . For a more complete description of the concentration-time curve, refer to Hubbard and others, 1982.

Dye-cloud traveltimes for each of the five test reaches are listed in table 3. Theoretically, when summing the traveltimes for individual test reaches, only the data for the traveltime of the centroid are truly additive. However, for the single injection and short distances used in each test reach, the traveltimes of the peaks and the centroids virtually are the same. The mean velocities of the peak and centroid for each of the test reaches also are listed in table 3. The mean test-reach velocities are almost identical whether calculated using peak traveltimes or centroid traveltimes.

Examining the dye-peak arrival times (table 3) at the first sampling cross section and the associated concentration-time curves (supplement 2) indicates that the Foxholm and Minot test reaches have the longest arrival times, 46.75 hours for the Foxholm reach and 23.25 hours for the Minot reach, and the flattest curves. The Velva and Towner test reaches have the shortest arrival times, 5.75 hours for the Velva reach and 4.75 hours for the Towner reach, and the sharpest curves. The Foxholm and Minot test reaches have the slowest mean velocities (about 0.06 and 0.05 ft/s) and the Velva test reach has the fastest (about 0.30 ft/s).

The long dye-cloud passage times at the first sampling cross sections in the Foxholm and Minot test reaches resulted in shortening the distance to the second sampling cross sections. Instead of the planned 4.0 river mi, the distance between the two sampling cross sections was shortened to 0.8 river mi for the Foxholm test reach and 0.9 river mi for the Minot test reach. Shortening the distance was necessary to ensure a detectable concentration of the gas tracer at the second sampling cross section because gas samples were being collected simultaneously with the dye samples.

Because of the shortened length of the Foxholm and Minot test reaches, test-reach velocities may not be representative of subreach velocities. To verify the representativeness of the test-reach velocities for all five of the subreaches, the respective dye clouds were located about a week later, and the peaks were located and sampled. The additional distances the dye traveled during the 7 to 8 d in the five subreaches ranged from about 6 to 25 mi. Using the longer distances, extended test-reach velocities were calculated and are listed in table 3. The extended test-reach

Table 3.--Data collected during traveltime measurements

[>indicates more than]

Site number <sup>1</sup>	River mile	Distance downstream from injection point (miles)	Cumulative traveltime of dye cloud beginning at injection (hours)			Dye-cloud passage time (hours)	Measured-peak dye concentration (micrograms per liter)	Mean velocity of dye cloud (foot per second)		Stream discharge (cubic feet per second)	Mean area under concentration-time curve (micrograms-hour factor per liter)	Dye correction factor	Dye recovery (percent)
			Leading edge	Peak	Trailing edge			Peak	Centroid				
<b>Foxholm test reach:</b> Continuous injection of 3.720 liters of 5-percent rhodamine-WT dye for 60 minutes beginning at 1700 hours, September 6, 1983													
5	413.8	0	--	--	--	--	--	--	--	--	--	--	--
	412.1	1.7	32.00	46.75	49.12	81.00	6.9	--	13.2	13.2	140	--	85
	411.3	2.5	48.00	65.25	68.07	101.00	6.1	0.06	13.8	13.8	132	1.06	80
	408.8	5.0	--	--	--	--	--	--	--	--	--	--	--
	2398.00	15.8	--	215.75	--	--	2.6	3.12	--	--	--	--	--
<b>Minot test reach:</b> Continuous injection of 2.855 liters of 5-percent rhodamine-WT dye for 60 minutes beginning at 0950 hours, September 7, 1983													
	390.5	0	--	--	--	--	--	--	10.5	--	--	--	--
	389.4	1.1	17.00	23.25	24.17	40.00	16	--	--	--	121	--	78
7	388.5	2.0	41.50	49.75	51.22	75.00	12	.05	11.0	11.0	116	1.04	75
	385.5	5.0	--	--	--	--	--	--	--	--	--	--	--
	2382.4	8.1	--	193.25	--	--	2.2	3.06	--	--	--	--	--
<b>Logan test reach:</b> Continuous injection of 2.800 liters of 5-percent rhodamine-WT dye for 30 minutes beginning at 0820 hours, September 14, 1983													
	363.9	0	--	--	--	--	--	--	12.0	12.0	--	--	--
9	362.6	1.3	15.50	17.00	17.18	21.00	14	--	20.0	20.0	569.4	--	585
	354.8	9.1	51.50	59.75	61.28	75.50	3.8	.27	32.0	32.0	40.7	1.08	79
	2330.0	33.9	--	191.00	--	--	--	3.27	--	--	--	--	--
<b>Velva test reach:</b> Continuous injection of 2.870 liters of 5-percent rhodamine-WT dye for 30 minutes beginning at 1125 hours, September 14, 1983													
	322.9	0	--	--	--	--	--	--	11.8	11.8	--	--	--
11	322.0	.9	3.50	5.75	5.95	11.00	53	--	15.0	15.0	100.7	--	90
	318.9	4.0	19.00	23.33	23.75	28.75	14	.26	25.0	25.0	53.2	1.14	79
	314.1	8.8	40.00	44.50	45.00	52.00	8.7	.33	27.0	27.0	46.3	1.05	75
	2293.4	29.5	--	190.75	--	--	2.7	3.23	--	--	--	--	--
<b>Towner test reach:</b> Continuous injection of 3.035 liters of 5-percent rhodamine-WT dye for 60 minutes beginning at 0810 hours, September 27, 1983													
	256.8	0	--	--	--	--	--	--	646.0	646.0	--	--	--
147	255.8	1.0	3.00	4.75	4.88	10.00	22	--	46.0	46.0	34.5	--	89
	250.3	6.5	29.50	34.75	35.52	44.00	5.0	.27	47.0	47.0	32.6	1.03	86
	2234.5	22.3	--	199.75	--	--	>.9	3.16	--	--	--	--	--

<sup>1</sup> Sites are part of synoptic sampling network for the waste-assimilation assessment.

<sup>2</sup> Extended test reach.

<sup>3</sup> Mean subreach velocity.

<sup>4</sup> Discharge estimated using digital record from stream-gaging stations 05117500 and 05120000, and measurements made during sampling.

<sup>5</sup> Synthesized, see supplement 4. (Actual dye recovery was 29 percent.)

<sup>6</sup> Discharge estimated using digital record from stream-gaging station 05122000 and measurements made during sampling.

<sup>7</sup> One mile upstream from synoptic sampling network site.

velocity almost equaled or equaled the test-reach velocity for the Minot and Logan subreaches, respectively; was greater than the test-reach velocity for the Foxholm subreach; and was less than the test-reach velocity for both the Velva and Towner subreaches. Based on the extended test-reach velocities, the mean velocity for the 186-river-mi study reach was 0.17 ft/s, or about a 67 d traveltime.

Traveltime-distance curves, which indicate the dye-cloud dispersion as it moves downstream and the channel uniformity, were prepared for each test reach (supplement 3). The leading and trailing edges, which represent the spread of the dye cloud, and the peak and centroid are indicated by each of the curves. The spread of the dye cloud is much greater for the Foxholm and Minot test reaches than for the Logan, Velva, and Towner test reaches, as indicated by the flatness of the Foxholm and Minot concentration-time curves.

The traveltime-distance curve for the Logan test reach indicates something unexpected that was not apparent from the concentration-time curves. It indicates a noticeable decrease in dependence of traveltime on distance at the 1.3-river-mi sampling cross section. This noticeable decrease indicates a nonuniformity in the test reach and a substantial decrease in traveltime in the test reach downstream from this sampling cross section. Additional sampling sites between the 1.3-river-mi sampling cross section and the 9.1-river-mi sampling cross section would have defined more precisely where the nonuniformity occurs in the test reach. Comparing the leading edge and passage traveltimes of the dye cloud in the Minot test reach to the leading edge and passage traveltimes of the dye cloud in the Logan test reach (the distance from the injection site to the first downstream sampling cross section is about the same for both, 1.1 river mi for the Minot test reach and 1.3 river mi for the Logan test reach), the leading edge arrival time is about the same for both (17.00 h for the Minot test reach and 15.50 h for the Logan test reach), yet the dye-cloud passage times are very different (23.00 h for the Minot test reach and only 5.50 h for the Logan test reach). In contrast to the Logan test reach, the uniformity of the Velva and Towner test reaches is indicated by the almost straight-line connection of the peak concentrations.

#### Adjustment to Measured Dye Concentrations

Measured dye concentrations need to be adjusted before they can have other uses; for example, making predictions in the magnitude of concentrations of waste discharged into the river. Initially the measured dye concentrations need to be adjusted for dye loss. So far, the discussion has assumed that the dye is conservative; that is, whatever dye is injected upstream will, after complete mixing, be recovered downstream. In practice, 100-percent dye recovery will not be realized. Dye loss is due to several causes, some of which are; adsorption to bottom and suspended sediment, photochemical decay, and chemical reaction (Hubbard and others, 1982). Measured dye concentrations adjusted for loss are called conservative dye concentrations. Measured dye concentrations adjusted to conservative dye concentrations are based on the percentage of

dye recovered at each sampling cross section downstream from the injection site within a test reach.

Dye-recovery percentages, as described by Hubbard and others (1982), were calculated at each sampling cross section for all test reaches. The percent recovery,  $R_p$ , for 5 percent rhodamine-WT, was computed as:

$$R_p = (0.1712) \frac{QAc}{Vol}, \quad (1)$$

where  $Q$  = the discharge at point of sampling, in cubic feet per second;  
 $Ac$  = the mean area under the total concentration-time curve, in micrograms-hours per liter, and represents the dye-cloud mass. These areas were computed by a digitizer and are listed in table 3; and  
 $Vol$  = the volume of 5-percent dye, in liters.

During calculation of the dye-recovery percentage, discharges at the first and second sampling cross sections of the Foxholm and Minot test reaches were disregarded because the distances between the cross sections were only a mile or less, and the discharge differences could have been due to the normal error expected when making a discharge measurement. Stream discharges for the Logan and Velva test reaches were estimated because of the rising river stage during dye-cloud sampling. Although discharge measurements were made during the dye-cloud sampling in the Logan and Velva test reaches, they were not made during the peak concentration. Estimates of discharge during measured-peak dye concentration were made from hourly discharges at the stream-gaging stations above Minot (station 05117500) and near Verendrye (station 05120000) and from measurements that were made during dye-cloud sampling. The discharge for the Towner test reach was estimated from the mean daily discharge at the stream-gaging station near Bantry (station 05122000) using a suitable lag time based on measured traveltime and velocity. The dye-recovery percentages are tabulated in table 3.

Dye-recovery percentages ranged from 75 to 90, except for the first sampling cross section in the Logan test reach where dye recovery was 29 percent, which was synthesized to 85 percent as explained below. The low percentage of dye recovery probably was because of nonrepresentative sampling of the dye cloud. Beginning about 6 h after injection, and continuing intermittently for about the next 24 h, the study area received about 1.5 in. of precipitation. A coulee (quantity of discharge from the rain is not known) discharges into the river about 50 yd upstream from the first sampling cross section in the Logan test reach. About 3 yd upstream from the sampling cross section, the flow in the river is divided into two channels; the majority of the flow is on the left side<sup>3</sup>, which also was the sampling cross section. Based on the long traveltime, it was assumed that the dye cloud was fairly well mixed at the point where the coulee

<sup>3</sup>The designation of a side or bank of a river as left or right is determined when one is looking downstream.

entered the river and that the coulee discharge diluted the dye cloud on the left side while the dye cloud on the right side remained undiluted. Because this test reach contains effluent from the municipal waste-stabilization pond at Minot, and some of the following calculations (for example, longitudinal-dispersion coefficient) require the area of the concentration-time curve, an attempt was made to synthesize the area under the concentration-time curve to represent a realistic dye recovery. The synthesis procedure is presented in supplement 4.

After calculating dye-recovery percentages, conservative dye concentrations were calculated. The concentration of a conservative solute can be computed from the measured dye concentration as follows:

$$C_{CON} = 100 \frac{C_{meas}}{R_p}, \quad (2)$$

where  $C_{CON}$  = conservative dye concentration (solute), in micrograms per liter;

$C_{meas}$  = measured dye concentration, in micrograms per liter; and

$R_p$  = percentage of dye recovered.

Of particular interest is the prediction of maximum (peak) concentrations, so if the measured-peak dye concentration is substituted in the above equation for the measured dye concentration, conservative-peak dye concentrations will be calculated. Conservative-peak dye concentrations are listed in table 4. For comparison of conservative-peak dye concentrations to measured-peak dye concentrations, the measured-peak dye concentrations are listed in table 3.

To compare longitudinal-dispersion characteristics among test reaches and to make predictions of peak solute concentrations at various sampling cross sections as the solute moves downstream, conservative-peak dye concentrations were converted to unit-peak dye concentrations. Unit solute concentration ( $C_u$ ) represents the response in 1 ft<sup>3</sup> of flow to 1 lb of conservative solute (Hubbard and others, 1982) and is computed by

$$C_u = \frac{C_{CON} \times Q}{W_d}, \quad (3)$$

where  $C_{CON}$  = the conservative solute concentration (dye), in micrograms per liter (if unit-peak concentrations were the concentration of interest, conservative-peak solute would be used); and

$W_d$  = the weight of pure dye injected, in pounds.

Unit dye concentration takes into consideration dye loss, differing discharges, and differing volumes of injected dye and isolates the effect longitudinal dispersion has in attenuating the peak concentrations with time and distance. Unit-peak dye concentrations were plotted against traveltime to create peak-attenuation curves (figs. 13 and 14), which can be used to make predictions of the magnitude and duration of solutes discharged into the river.

Table 4.--Conservative-peak and unit-peak dye concentrations

Test reach	River mile	Conservative-peak dye concentration (micrograms per liter)	Weight of pure dye injected		Unit-peak dye concentration	
			(pound)	(kilogram)	(micrograms per liter times cubic feet per second per pound)	(micrograms per liter times cubic meters per second per kilogram)
Foxholm	413.8	--	0.49	0.22	--	--
	412.1	8.1	--	--	220	14
	411.3	7.6	--	--	210	13
Minot	390.5	--	.37	.17	--	--
	389.4	20.5	--	--	600	37
	388.5	16.0	--	--	470	29
Logan	363.9	--	.37	.17	--	--
	362.6	48.0	--	--	2,610	161
	354.8	4.8	--	--	420	26
Velva	322.9	--	.38	.17	--	--
	322.0	58.9	--	--	2,320	145
	318.9	17.7	--	--	1,160	74
	314.1	11.6	--	--	820	49
Towner	256.8	--	.40	.18	--	--
	255.8	24.7	--	--	2,840	177
	250.3	5.8	--	--	680	43

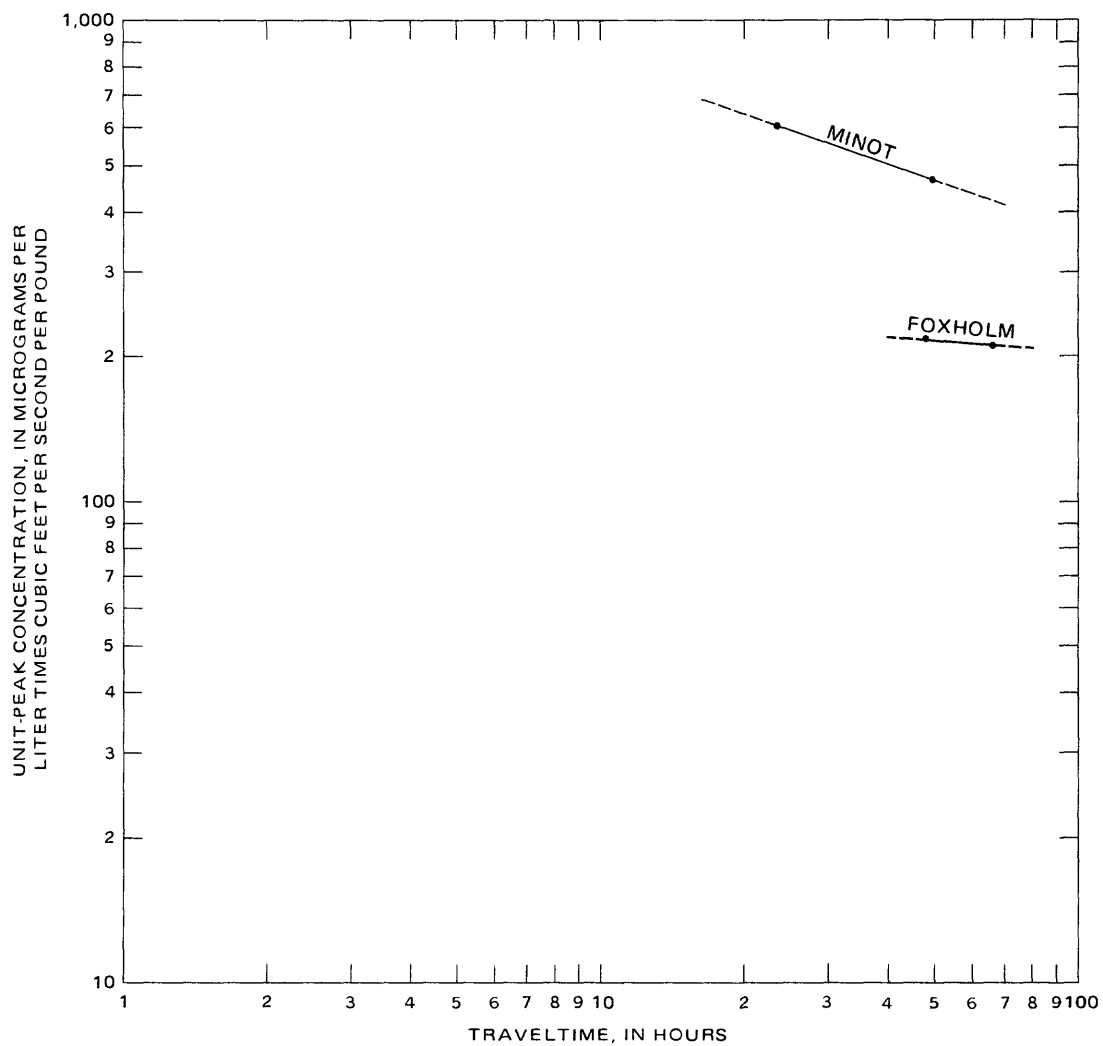
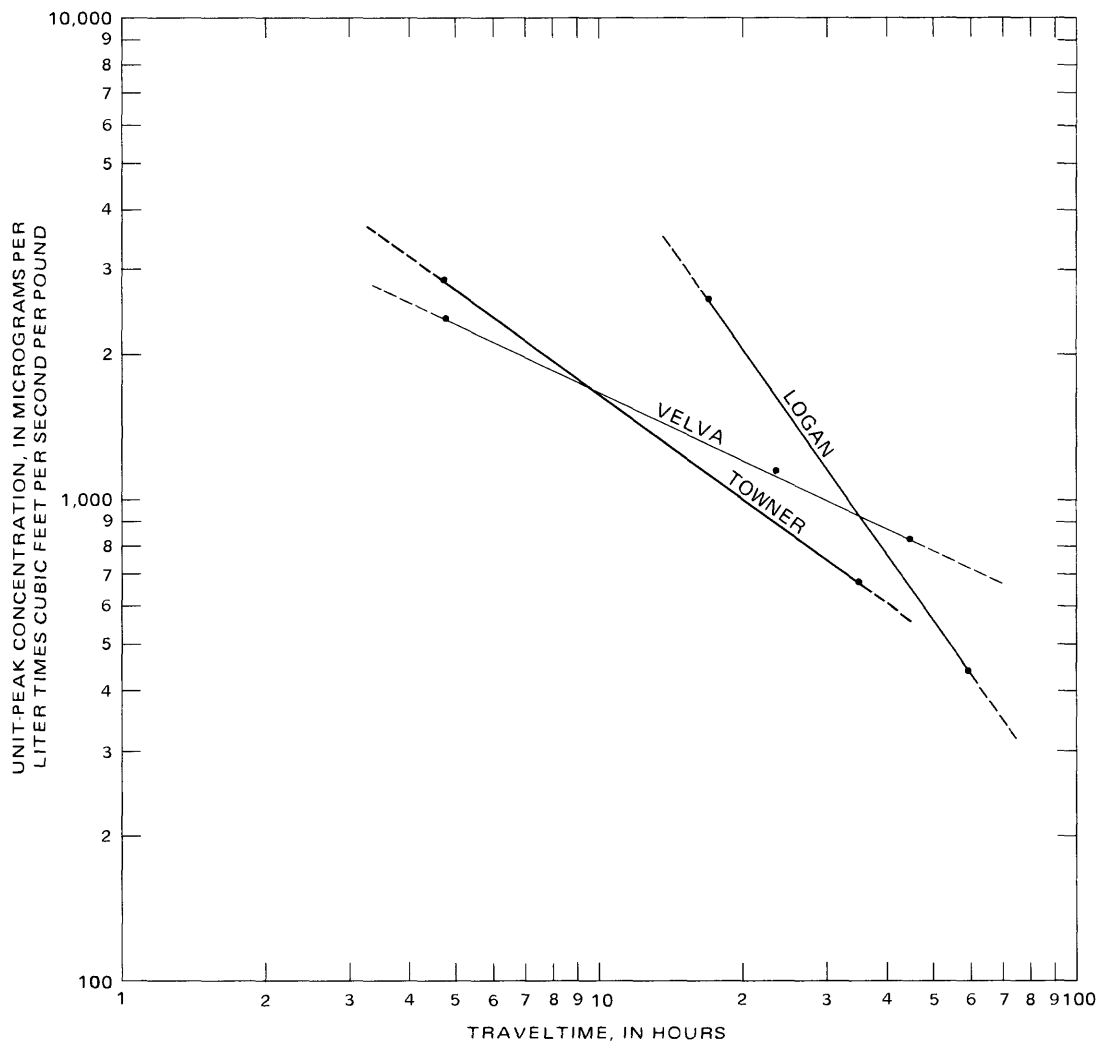


Figure 13.—Attenuation of unit-peak concentrations with traveltime for: Foxholm test reach, September 6-11, 1983; and Minot test reach, September 7-10, 1983.



**Figure 14.—Attenuation of unit-peak concentrations with traveltime for: Logan test reach, September 14-17, 1983; Velva test reach, September 14-16, 1983; and Towner test reach, September 27-29, 1983.**

Unit-peak dye concentrations are shown in table 4 and are plotted by test reach on log-log paper in supplement 5. In addition to unit-peak dye concentration, measured- and conservative-peak dye concentrations also are plotted in supplement 5. (Note that the unit-peak dye concentrations in supplement 5 are expressed in micrograms per liter times cubic meters per second per kilogram; whereas, unit-peak concentrations in figures 13 and 14 are expressed in micrograms per liter times cubic feet per second per pound. The different units were used in supplement 5 so that the unit-peak dye concentrations could be plotted on the same scale as the measured- and conservative-peak dye concentrations, which are expressed in micrograms per liter.)

According to Yotsukura and Sayre (Hubbard and others, 1982, p. 34), after initial mixing, the graph of the conservative-peak dye concentration plotted against traveltime tends to be a straight line on log-log paper. Because the number of sampling cross sections in four of the test reaches was limited to two, a straight-line plot for these test reaches is assumed. However, this limitation does not apply to the Velva test reach, which had three sampling cross sections, and the three values for the conservative-peak dye concentration do plot as a straight line. Taking into consideration this limitation in the data, but using the straight-line plot for the Velva test reach as a confirmation of Yotsukura and Sayre's statement, the assumption is that the straight-line plots for the five test reaches are valid, but the slopes of the straight-line plots may have some error.

Plotting the measured, conservative, and unit peaks on the same log-log paper allows for comparing the difference in the percentage of dye recoveries and the change in stream discharge among the sampling sites. The slopes of the lines for the Minot and Towner test reaches are nearly parallel, indicating a small change in the difference of percentage of dye recovery (3 percent for each test reach) and an almost constant stream discharge (10.5 to 11.0 ft<sup>3</sup>/s for the Minot reach and 46 to 47 ft<sup>3</sup>/s for the Towner reach) between sampling sites 1 and 2. The other three test reaches had larger changes in the difference of percentage of dye recoveries (ranging from 79 to 85 percent for the Logan test reach and 75 to 90 percent for the Velva test reach) and, with the exception of the Foxholm, test reach, had a larger increase in stream discharge (ranging from 12.0 to 32.0 ft<sup>3</sup>/s for the Logan test reach and from 11.8 to 27.0 ft<sup>3</sup>/s for the Velva test reach). The almost constant stream discharge for the Foxholm test reach is indicated by the almost parallel lines between the plot of the conservative peaks and the unit-concentration peaks.

To make comparisons of and distinctions in the longitudinal-dispersion characteristics of the five test reaches, the peak-attenuation curves for the Foxholm and Minot reaches are plotted in figure 13; and for the Logan, Velva, and Towner reaches they are plotted in figure 14. The slope of the peak-attenuation curve is an indication of the longitudinal-dispersion efficiency of the channel (Hubbard and others, 1982). Longitudinal-dispersion efficiency is characterized by the ability of a channel to disperse a solute through a reach. The greater the longitudinal-dispersion efficiency, the greater the decrease of the peak concentration

during a given time. Longitudinal-dispersion efficiency varies directly with the slope of the curve. In order of decreasing channel dispersing efficiency, the test reaches are: Logan, Towner, Velva, Minot and Foxholm. The Logan, Towner, Velva, and Minot test reaches have the most efficient dispersing channels and the Foxholm test reach has the least efficient dispersing channel. To quantify the dispersion efficiency of a channel, longitudinal-dispersion coefficients were calculated.

Longitudinal-dispersion coefficients were computed for all five test reaches. A longitudinal-dispersion coefficient represents the rate at which a stream dilutes a soluble substance by mixing it into an ever increasing volume of water as the solute cloud lengthens. The calculations used to compute a longitudinal-dispersion coefficient are based on a change-of-moment method, which is described by Fischer (1966). The basic equation used is as follows:

$$K_x = \frac{(\bar{U})^2}{2} \cdot \frac{\sigma^2_{t_2} - \sigma^2_{t_1}}{\bar{t}_2 - \bar{t}_1}, \quad (4)$$

where  $K_x$  = longitudinal-dispersion coefficient, in square feet per second;

$\bar{U}$  = mean peak velocity, in feet per second;

$\sigma^2_{t_2}$  = the variance of the concentration-time curve at the downstream sampling cross section, in hours squared;

$\sigma^2_{t_1}$  = the variance of the concentration-time curve at the upstream sampling cross section, in hours squared; and

$\bar{t}_2, \bar{t}_1$  = the mean time of passage of the tracer cloud (centroid) past each sampling cross section, in hours.

The variance and centroid were computed by a program provided by R.E. Rathbun (U.S. Geological Survey, written commun., 1985). The program initially computes the areas under the dye curves by summing the trapezoids formed under the curve after the concentration-time coordinates are connected by a straight line. The areas and centroids calculated by this program (table 5) are similar to the digitizer-calculated areas (table 3).

The only restriction for using the above equation to calculate longitudinal-dispersion coefficients is that the first sampling cross section needs to be sufficiently downstream so that the dye concentration is approximately uniform in the lateral direction. Fischer (1968) determined that the above equation resulted in an approximation of the longitudinal-dispersion coefficient if the mixing time (in hours) was greater than

$$\frac{(1.8) L^2}{H U^*}, \quad (5)$$

Table 5.--Area, centroid, and variance of concentration-time data computed by computer program and longitudinal-dispersion coefficients and mixing times for test reaches, September 1983

Test reach	Concentration-time data					
	River mile	Mean area under dye curve (micrograms-hour per liter)	Centroid cumulative traveltime beginning at leading edge of dye cloud (hours)	Variance (hour squared)	Longitudinal-dispersion coefficient (square feet per second)	Mixing time (hours)
Foxholm	412.1	141	18.47	80.4	--	1.3
	411.3	132	37.51	99.18	7.1	--
Minot	389.4	122	7.82	14.35	--	.9
	388.5	118	35.78	35.91	4.2	--
Logan	362.6	<sup>1</sup> 69.4	1.72	.72	61	1.4
	354.8	40.7	45.86	20.64	--	--
Velva	322.0	103	2.54	1.08	--	1.2
	318.9	52	20.25	2.59	22	--
	314.1	45	41.68	4.75	23	--
Towner	255.8	34.5	1.69	.95	--	2.7
	250.3	32.9	31.50	9.63	36	--

<sup>1</sup>Synthesized, see supplement 4.

where  $L$  = distance from the point of maximum surface velocity to the farthest bank, about one-half the stream width, in feet;

$H$  = hydraulic depth, in feet; and

$U^*$  = shear velocity, in feet per second.  $U^*$  is defined as  $\sqrt{g H S}$ : where  $g$  is acceleration because of gravity [32.2 (ft/s)/s]; and  $S$  is the slope of the energy gradient, in foot per foot.

The theoretical mixing times required to obtain approximately uniform dye concentration in the lateral direction for the various test reaches are listed in table 5. In all instances, the leading-edge arrival time (table 3) was greater than the mixing time, yet at the first Velva and Towner sampling cross sections, the dye was not uniformly mixed.

The longitudinal-dispersion coefficients (table 5) range from 4.2 to 61 ft<sup>2</sup>/s. The Logan test reach had the largest longitudinal-dispersion coefficient, 61 ft<sup>2</sup>/s, and the Minot test reach had the smallest, 4.2 ft<sup>2</sup>/s.

#### Uses of Dispersion Data

An aspect of dispersion that has practical application is the attenuation in the peak solute concentration as it moves downstream. Peak-attenuation curves are used as predictive methods to estimate the peak concentration of a spilled substance at some point downstream.

An example of how to use the unit-peak concentration curves for prediction purposes is as follows: Assume 1,000 lb of a conservative substance is spilled into the Souris River from the North Dakota Highway 14 bridge north of Towner, N. Dak., at river mi 256. The problem is how to predict the arrival time and magnitude of the peak concentration at the entrance of J. Clark Salyer National Wildlife Refuge at river mi 228, a distance of 28 river mi. Further assume the stream discharge in this 28-river-mi reach is 45 ft<sup>3</sup>/s and the mean velocity is 0.26 ft/s. At a rate of 0.26 ft/s, it would require about 160 h to travel the 28 river mi. To calculate the concentration of the peak, find 160 h in figure 14, go to the Towner curve, and at the intersection of the Towner curve with 160 h pick the unit value of 225 µg/L x (ft<sup>3</sup>/s)/lb. The peak solute concentration,  $C_p$ , using the method of Hubbard and others (1982), would be:

$$C_p = 225 \text{ } \mu\text{g/L} \times \frac{\text{ft}^3/\text{s}}{\text{lb}} \times \frac{1,000 \text{ lb}}{45 \text{ ft}^3/\text{s}} = 5,000 \text{ } \mu\text{g/L}.$$

These predictive methods only apply to a conservative substance after complete mixing has occurred. If a spill involves an insoluble or immiscible substance like oil, the predicted peak concentration may be greater than for a conservative substance completely mixed in the flow. Also, if a substance is nonconservative, such as dissolved gases, nutrients, or other substances that can be biologically or chemically degraded or affected by other physical processes, then the predictive methods discussed above would indicate only the maximum concentration at the downstream point. The actual concentration for nonconservative substances would be decreased by the actions of these other processes.

#### Reaeration Results

Mean reaeration coefficients were determined for each of the five test reaches using the peak method of Rathbun and others (1975). Reaeration coefficients were converted from desorption coefficients, which were calculated using peak concentrations of the tracer gases and the dye after adjustment for dye loss. The equation for the tracer-gas desorption coefficient ( $K_G$ ) for the test reach between sampling cross sections 1 (upstream) and 2 (downstream) is:

$$K_{g1-2} = \frac{1}{t_2 - t_1} \ln \frac{C_{g1} / C_{d1}}{C_{g2} / (C_{d2} J_2)} \quad (6)$$

where  $\ln$  = natural logarithm, base  $e$ ;

$C_{g1}$ ,  $C_{g2}$  = peak concentration of the tracer gas at the upstream and downstream sampling cross sections, respectively, in micrograms per liter;

$C_{d1}$ ,  $C_{d2}$  = peak concentration of dye at the upstream and downstream sampling cross sections, respectively, in micrograms per liter;

$t_2$ ,  $t_1$  = traveltime of the peak concentrations of dye at the downstream and upstream sampling cross sections, respectively, in hours; and

$J_2$  = dye-loss correction factor between the upstream and downstream sampling cross sections.

Because rhodamine-WT dye is not completely conservative in streams, the area under the concentration-time curve needs to be corrected for dye loss and for any significant flow accrual that occurred before the desorption coefficients are computed. Dye-correction factors were calculated for each of the test reaches by using a ratio of the upstream dye-recovery percentage to the downstream dye-recovery percentage. For example, in the Foxholm test reach, 85 percent of the dye was recovered at the upstream sampling cross section and 80 percent of the dye was recovered at the downstream sampling cross section for a dye-correction factor of  $85/80 = 1.06$ . The dye-correction factors listed in table 3 are quite uniform, varying only from 1.03 to 1.06, except for the Logan test reach (1.08) and the Velva test reach (1.14). The dye-correction factor for the Logan test reach is synthetic as a result of reconstructing the area under the concentration-time curve as explained in supplement 4. The larger dye-correction factor for the Velva test reach probably is because of the increase in stream discharge resulting from the precipitation received after injection.

The desorption coefficient is converted to a reaeration coefficient ( $K_2$ , base  $e$  logarithmic units) using the relation:

$$K_2 = RK_g \quad (7)$$

where  $R$  = the ratio of the absorption coefficient for oxygen to the desorption coefficient for the tracer gas (determined in the laboratory).

From laboratory studies by Rathbun and others (1978), the following relations have been determined:

$$\text{Ethylene, } K_2 = 1.15K_g,$$

and

$$\text{Propane, } K_2 = 1.39K_g.$$

The peak concentrations and traveltimes of peak concentrations for the ethylene and propane gas tracers and rhodamine-WT dye are given in table 6. These concentrations and traveltimes, and the dye-correction factors

Table 6.--Peak concentrations and traveltime of peak concentrations for ethylene and propane tracer gases and rhodamine-WT dye, September 1983

Test reach	River mile	Peak concentration (micrograms per liter)			Traveltime of peak concentrations (hours)		
		Ethylene	Propane	Dye	Ethylene	Propane	Dye
Foxholm	412.1	4.1	5.7	6.9	44.33	44.33	46.75
	411.3	.9	3.5	6.1	63.67	63.67	65.25
Minot	389.4	21	15	16	22.67	23.00	23.25
	388.5	9.4	8.7	12	49.00	49.67	49.75
Logan	362.6	16	8.4	14	17.00	17.00	17.00
	354.8	.8	1.1	3.8	59.50	59.50	59.75
Velva	322.0	62	33	53	5.75	5.75	5.75
	318.9	4.4	4.4	14	23.00	23.00	23.33
	314.1	.6	1.2	8.7	43.75	43.75	44.50
Towner	255.8	63	36	22	4.75	4.75	4.75
	250.3	4.1	4.6	5.0	34.50	34.75	34.75

listed in table 3 were used in the peak method of the reaeration-coefficient computation. The reaeration coefficients at measured water temperatures were adjusted to a common temperature base of 20 °C by the following formula (Elmore and West, 1961):

$$K_2(20\text{ }^\circ\text{C}) = K_2(t) (1.0241)^{20-t},$$

where  $t$  = mean test-reach water temperature, in degrees Celsius.

#### Experimental Values

The mean temperatures for water in the test reaches and reaeration coefficients are given in table 7. The reaeration coefficients, adjusted to a common 20 °C base, ranged from 0.62 to 2.45 per day for ethylene and from 0.39 to 1.66 per day for propane. In all instances, the ethylene  $K_2$  values are larger than the propane  $K_2$  values, ranging from about 1.5 to 2.8 times larger. These large differences do not appear random, and suggest that some of the assumptions inherent to the modified tracer technique are being violated.

According to Kilpatrick and others (1987), the assumption that removal of gas by desorption only and that no other physical, chemical, or biological processes interfere is not valid in this case particularly because of the long travel time (see table 3). The long travel times enhance the

Table 7.--Reaeration coefficients ( $K_2$ ) for ethylene and propane determined using peak computation methods, September 1983

Test reach	Mean water temperature (degrees Celsius)	$K_2$ at measured water temperatures (day <sup>-1</sup> )		$K_2$ adjusted to 20 °Celsius (day <sup>-1</sup> )	
		Ethylene <sup>1</sup>	Propane	Ethylene <sup>1</sup>	Propane
		Foxholm	18.3	2.17	0.76
Minot	17.0	.58	.37	.62	.39
Logan	13.0	1.14	.63	1.35	.74
Velva	12.5	2.05	1.39	2.45	1.66
Towner	14.5	1.19	.68	1.35	.78

<sup>1</sup>The ethylene  $K_2$  values are shown for comparative purposes and are not considered representative of the test reach.

probability of biodegradation. Also, ethylene, which is an unsaturated hydrocarbon, is more chemically reactive than saturated hydrocarbons like propane. As a result, the ethylene  $K_2$  values are larger than the propane  $K_2$  values. The ethylene  $K_2$  values are shown in table 7 only for comparative purposes and are not considered to be representative of the  $K_2$  values in the test reach. The propane  $K_2$  values are considered representative of the test reach and could be used in the modeling study.

Based on mean velocity and depth, the Foxholm and Minot test reaches are quite similar and were expected to have the smallest and similar propane  $K_2$  values; however, the propane  $K_2$  values for the Foxholm test reach (0.79 per day) is about twice as large as the  $K_2$  values for the Minot test reach (0.39 per day). The larger propane  $K_2$  value for the Foxholm test reach may be attributed to the greater number of farmer- or rancher-built crossings that exist in the Foxholm test reach as compared to the Minot test reach. Reaeration may be enhanced in the crossing areas because the water is more turbulent, flowing over the crossing and falling over the drop on the downstream side of the crossing. The Velva test reach has the largest propane  $K_2$  value, it also had the fastest mean velocity and the shallowest mean depth.

#### Predictive-Equation Values

To determine which predictive equations produced reaeration coefficients similar to the experimental (measured) reaeration coefficients and which are applicable to the Souris River, calculations were made for 10 empirical and 8 semiempirical equations. These predictive equations were evaluated by Rathbun (1977) and are shown by authorship in tables 8 and 9. Empirical equations generally have a reaeration coefficient

Table 8.--Comparison of reaeration coefficients determined using measured data (September 1983) with those determined using velocity-depth (empirical) equations

Method	Reaeration coefficients (per day) base e units for indicated test reach				
	Foxholm	Minot	Logan	Velva	Towner
<u>Determined using measured data</u>					
Based on propane	0.79	0.39	0.74	1.66	0.78
<u>Determined using velocity-depth equations from:</u>					
O'Connor and Dobbins (1958)	0.70	0.54	1.6	2.7	1.5
Churchill and others (1962)	.15	.11	.69	1.3	.63
Owens and others (1964) <sup>1</sup>	.53	.38	1.7	3.2	1.6
Owens and others (1964) <sup>2</sup>	.53	.38	1.6	3.0	1.5
Langbein and Durum (1967)	.13	.09	.61	1.0	.56
Isaacs and Gaudy (1968)	.12	.09	.58	1.0	.53
Negulescu and Rojanski (1969)	.47	.37	1.7	2.5	1.6
Padden and Gloyna (1971)	.36	.28	1.1	1.6	.0
Bennett and Rathbun (1972)	.70	.51	1.9	3.4	1.8
Bansal (1973)	.22	.17	.59	1.0	.55

$${}^1K_2 = 1.09 U^{0.73}/H^{1.75}.$$

$${}^2K_2 = 1.02 U^{0.67}/H^{1.85}.$$

directly proportional to the mean flow velocity and inversely proportional to the mean flow depth. Semiempirical equations are based on the rate of energy dissipation. The information that was necessary to make the predictive-equation calculations is given in table 10. A comparison of the propane experimental (measured) reaeration coefficients to the predicted reaeration coefficients is given in tables 8 and 9. A majority (more than 60 percent) of the predicted equations produced reaeration coefficients that were smaller than the experimental coefficients.

An error analysis, as used by Rathbun (1977), was performed on the predictive-equation reaeration coefficients. A listing of the errors of estimate is given in table 11. The listing in table 11 does not include the error analysis results of Lau's (1972) semiempirical equation because they were considered outliers and had a mean absolute error of estimate of 157. The error of estimate (PE) is defined as:

$$PE = (K_2 \text{ pred} - K_2 \text{ exp})/K_2 \text{ exp}, \quad (8)$$

Table 9.--Comparison of reaeration coefficients determined using measured data (September 1983) with those determined using energy-dissipation (semiempirical) equations

Method	Reaeration coefficients (per day) base e units for indicated test reach				
	Foxholm	Minot	Logan	Velva	Towner
<u>Determined using measured data</u>					
Based on propane	0.79	0.39	0.74	1.66	0.78
<u>Determined using energy-dissipation equations from:</u>					
Churchill and others (1962)	0.001	0.0008	0.09	0.30	0.20
Krenkel and Orlob (1963)	1.1	.83	2.0	2.6	1.2
Cadwallader and McDonnell (1969)	.39	.26	.79	1.1	.41
Thackston and Krenkel (1969)	2.0	1.5	1.8	2.2	1.0
Bennett and Rathbun (1972)	.76	.54	1.4	2.3	.97
Lau (1972)	425	294	15	11	3.3
Parkhurst and Pomeroy (1972)	.24	.17	.41	.59	.25
Tsivoglou and Neal (1976)	.04	.02	.20	.23	.06

where  $K_2$  pred = reaeration coefficient predicted by equations, and  
 $K_2$  exp = reaeration coefficient measured experimentally.

To calculate the mean error of estimate, absolute values are used in the computation because individual error values can be either negative or positive. The results of the error-of-estimate analysis indicate that none of the equations produced consistent, small errors of estimate for each of the five test reaches. The lowest mean error of estimate for all five test reaches was 0.35, which was produced by the Cadwallader and McDonnell (1969) equation. The range of error of estimate for this equation was -0.51 to 0.07. In other words, if this equation were applied to all of the whole test reaches, one would be 35 percent off in predicting the reaeration coefficient. A better approach, which would reduce the amount of error, would be to select a predictive equation for each test reach that produced the lowest error of estimate for that test reach. For instance, the Bennett and Rathbun (1972) energy-dissipation equation had the lowest absolute error of estimate (0.04) of all the predictive equations in the Foxholm test reach. For the Minot test reach, both Owens

Table 10.--Geometry of test reaches and traveltime and velocity data collected in the test reaches during September 1983

Test reach	Geometry			Traveltime data		Velocity data		
	Decrease in elevation of thalweg <sup>1</sup> (feet)	Length <sup>2</sup> (feet)	Slope (S) (foot per foot)	Mean hydraulic depth of water (H) <sup>2</sup> (feet)	Traveltime of peak concentration of dye (hours)	Mean velocity of peak concentration of dye (U) (foot per second)	Shear velocity (U*) (foot per second)	Froude number (F)
Foxholm	0.6	4,200	1.42x10 <sup>-4</sup>	2.9	18.50	0.06	0.12	0.0065
Minot	.5	4,800	1.00x10 <sup>-4</sup>	3.3	26.50	.05	.10	.0052
Logan	5.0	41,200	1.21x10 <sup>-4</sup>	2.6	42.75	.27	.10	.0285
Velva	5.2	41,700	1.25x10 <sup>-4</sup>	2.0	38.75	.30	.09	.0374
Towner	1.0	29,000	.34x10 <sup>-4</sup>	2.8	30.00	.27	.06	.0272

<sup>1</sup>Water surface profile, Souris River, North Dakota (from U.S. Army Corps of Engineers, St. Paul District, written commun., 1970).

<sup>2</sup>The test-reach length and mean hydraulic depth differ from the length and mean hydraulic depth shown in table 2. The length here is the distance between the sampling cross sections. The change in length necessitated an adjustment in the mean hydraulic depth. Also, the mean hydraulic depth was adjusted further to indicate the depth of flow at the time the tracers were sampled.

Table 11.--Error analysis of reaeration coefficients

[Based on comparisons presented in tables 8 and 9 between reaeration coefficients determined using measured data (September 1983) and those determined using velocity-depth (empirical) and energy-dissipation (semiempirical) equations]

Method	Error of estimate for indicated test reach					Mean of absolute value of error of estimate
	Foxholm	Minot	Logan	Velva	Towner	
<u>Determined using velocity-depth equations from:</u>						
O'Connor and Dobbins (1958)	-0.11	0.38	1.16	0.63	0.92	0.63
Churchill and others (1962)	-.81	-.72	-.07	-.22	-.19	.41
Owens and others (1964) <sup>1</sup>	-.33	-.03	1.30	.93	1.05	.72
Owens and others (1964) <sup>2</sup>	-.33	-.03	1.16	.81	.92	.64
Langbein and Durum (1967)	-.82	-.77	-.18	-.40	-.28	.49
Isaacs and Gaudy (1968)	-.85	-.77	-.22	-.40	-.32	.51
Negulescu and Rojanski (1969)	-.41	-.05	1.30	.50	1.05	.66
Padden and Gloyna (1971)	-.54	-.28	.49	-.04	.28	.49
Bennett and Rathbun (1972)	-.11	.31	1.57	1.05	1.31	.86
Bansal (1973)	-.72	-.56	-.20	-.40	-.29	.44
<u>Determined using energy-dissipation equations from:</u>						
Churchill and others (1962)	-1.00	-1.00	-.88	-.82	-.74	.89
Krenkel and Orlob (1963)	.39	1.13	1.70	.57	.54	.86
Cadwallader and McDonnell (1969)	-.51	-.33	.07	-.34	-.47	.35
Thackston and Krenkel (1969)	1.53	2.85	1.43	.33	.28	1.28
Bennett and Rathbun (1972)	-.04	.38	.89	.38	.24	.38
Parkhurst and Pomeroy (1972)	-.70	-.56	-.45	-.64	-.68	.61
Tsivoglou and Neal (1976)	-.95	-.95	-.73	-.86	-.92	.88

$$^1K_2 = 1.09 U^{0.73}/H^{1.75}.$$

$$^2K_2 = 1.02 U^{0.67}/H^{1.85}.$$

and others (1965) velocity-depth equations had the lowest absolute error of estimate (0.03). In the Logan test reach, the Churchill and others (1962) velocity-depth equation and the Cadwalller and McDonnell (1969) energy-dissipation equation had the lowest absolute error of estimate (0.07). In the Velva test reach it was Padden and Gloyna (1971) velocity-depth equation (0.06). In the Towner test reach, none of the predictive equations had estimates of error in the range (0.03-0.07) of the other four test reaches; the lowest absolute error of estimate resulted from the Churchill and others (1962) velocity-depth equation (0.19). These results demonstrate the difficulty in using a predictive equation that will produce a reaeration coefficient that is representative of the entire subreach instead of measuring the reaeration coefficient.

#### SUMMARY

The North Dakota State Department of Health made an appraisal of the Souris River water quality during 1976-78 for the North Dakota Statewide 208 Water Quality Management Plan. Their appraisal indicated some degradation had occurred along some reaches of the river since 1967. To determine the causes for the water-quality degradation, they requested a water-quality assessment of the Souris River.

This report addresses the second objective of the Souris River water-quality assessment; namely determination of low-flow traveltime, longitudinal-dispersion, and reaeration characteristics of a 186-mile reach of the Souris River. These characteristics could be used as data for use in a mathematical model that estimates the waste-assimilation capacity of the river.

The Souris River is an international river draining parts of the United States and Canada. About 360 miles of the total length (790 miles) of the river is located in the United States. The study reach consists of the part of the Souris River from Lake Darling Dam to J. Clark Salyer National Wildlife Refuge. At low flow, the study reach is 186 river miles in length.

Dye- and gas-tracing techniques were used to determine low-flow traveltime, longitudinal-dispersion, and reaeration characteristics. This tracer study was conducted during September 1983 to coincide with low flow in the river under open-water conditions. Arrangements were made with the U.S. Fish and Wildlife Service to decrease stream discharge and maintain a flow of 10 cubic feet per second from Lake Darling for 5 weeks beginning August 22, 1983. During September, flow in the Souris River can be expected to exceed 10 cubic feet per second about 60 percent of the time. Flows in the downstream part of the study reach were expected to range from 20 to 30 cubic feet per second; however, about midway through the test about 1.0 to 1.5 inches of precipitation fell, and flows ranged from 10.5 cubic feet per second in the upper part of the study reach to 47.0 cubic feet per second in the lower part. The precipitation occurred after tracer injection in the Logan and Velva test reaches and may have had an adverse effect on some of the results from these test reaches.

In the study reach, the Souris River drains an area that predominantly produces agricultural products. The river flows slowly within its almost flat-sloped, meandering channel, which has been modified by human and animal activities. Because the physical and hydraulic characteristics of the river change along the study reach, it was divided into five subreaches that ranged from 18 to 55 river miles in length. These subreaches are, Foxholm, Minot, Logan, Velva, and Towner. Eight photographs show the characteristic features of the subreaches. Within each subreach, a representative test reach that ranged from 5.0 to 9.1 river miles in length was selected for injection of rhodamine-WT dye and low-molecular-weight hydrocarbon gases as tracers. Stream widths were measured at the beginning and end of each test reach and at every mile point inbetween. Soundings were made at either 2- or 5-foot intervals at each cross section to define the depth profile. The range of maximum width was 30 to 90 feet and the range of maximum depth was 1.4 to 8.4 feet. Plots of each cross section were made and all the plots within each test reach are shown as a perspective plot.

Traveltime and longitudinal-dispersion characteristics were measured using standard fluorometric techniques and reaeration characteristics were measured using a modified tracer technique. A solution of 5-percent rhodamine-WT dye and ethylene and propane gas were used as tracers. Samples were collected from at least two sampling cross sections in each test reach. Dye samples were collected to define the entire concentration range; gas samples were collected to define the peak concentration only. Dye-recovery percentages were calculated for each sampling cross section and ranged from 75 to 90 percent.

Concentration-time, traveltime-distance, and unit-peak dye-concentration curves were prepared for each test reach. The concentration-time curves indicate the Foxholm and Minot test reaches have the longest dye-peak arrival times and the flattest curves; the Towner test reach has the shortest dye-peak arrival time and the sharpest curve, followed by the Velva test reach. The traveltime-distance curves indicate the test reaches are fairly uniform in traveltime, except the Logan test reach where traveltime decreased within the test reach. Mean velocities in the test reaches ranged from 0.05 foot per second in the Minot test reach to 0.30 foot per second in the Velva test reach. For the 186-mile study reach, the mean velocity was 0.17 foot per second, or a traveltime of about 67 days. The unit-peak dye concentration curves indicate that in order of decreasing magnitude the Logan, Towner, and Velva test reaches have the greater dispersion efficiency. Longitudinal-dispersion coefficients calculated for each test reach ranged from 4.2 square feet per second in the Minot test reach to 61 square feet per second in the Logan test reach.

The measured test-reach ethylene reaeration coefficients were disregarded because the loss of ethylene was much greater than for propane. The difference suggests some additional action was causing loss of ethylene that was not affecting the propane. Ethylene reaeration coefficients were from about 1.5 to 2.8 times greater than propane reaeration coefficients. Measured test-reach propane reaeration coefficients, adjusted

to 20 °C, ranged from 0.39 per day in the Minot test reach to 1.66 per day in the Velva test reach. The measured propane reaeration coefficients were compared with reaeration coefficients calculated using 10 empirical and 9 semiempirical predictive equations. The lowest mean error of estimate for all five test reaches was 0.35, which was produced by the Cadwallader and McDonnell (1969) equation. The range of error of estimate for this equation was -0.51 to 0.07. To reduce this error, a predictive equation that produces the lowest error of estimate should be selected for each test reach to calculate reaeration coefficients.

#### SELECTED REFERENCES

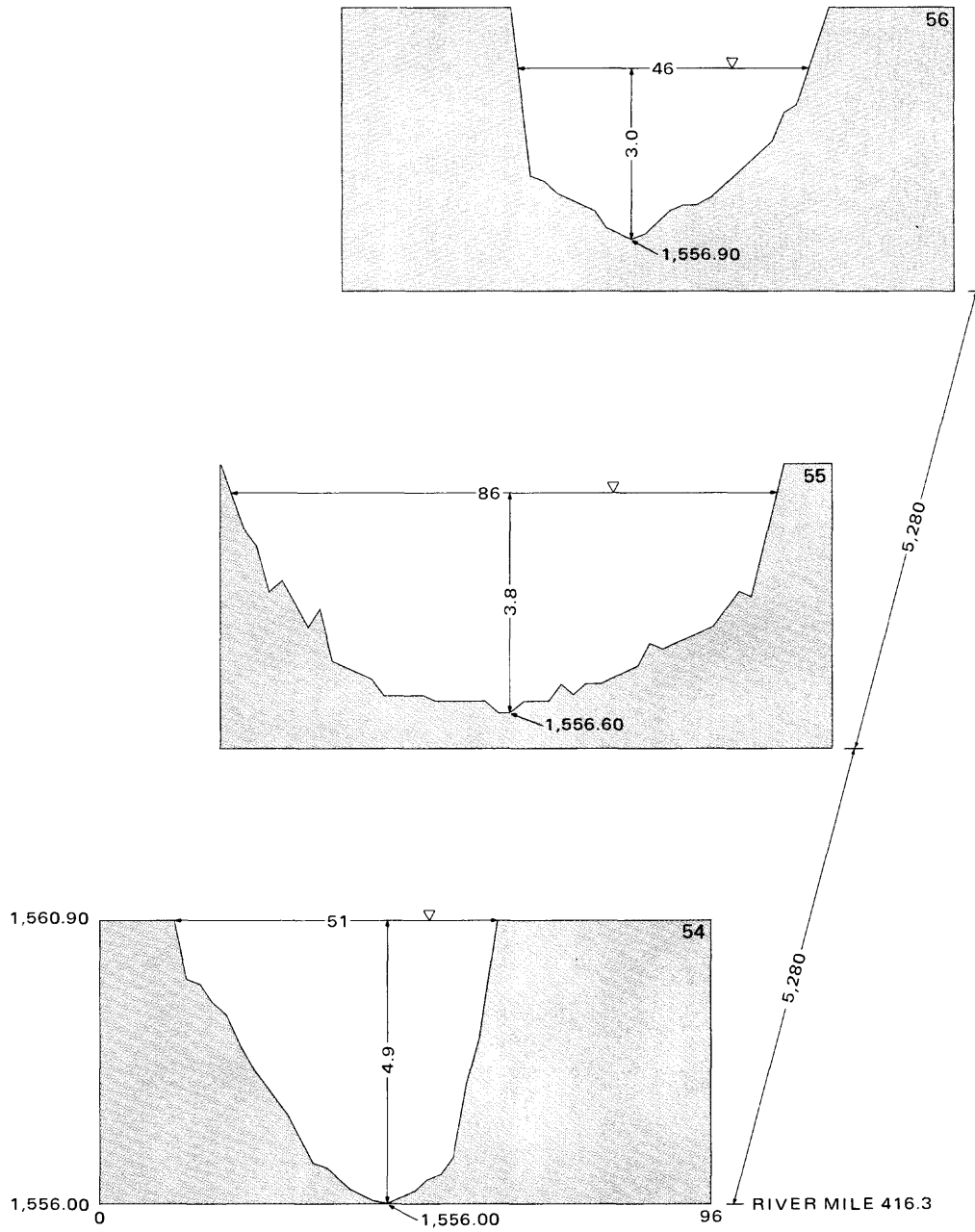
- Bansal, M.K., 1973, Atmospheric reaeration in natural streams: *Water Research*, v. 7, no. 5, p. 769-782.
- Bennett, J.P., and Rathbun, R.E., 1972, Reaeration in open-channel flow: U.S. Geological Survey Professional Paper 737, 75 p.
- Cadwallader, T.E., and McDonnell, A.J., 1969, A multivariate analysis of reaeration data: *Water Research*, v. 3, p. 731-742.
- Churchill, M.A., Elmore, H.L., and Buckingham, R.A., 1962, The prediction of stream reaeration rates: American Society of Civil Engineers, *Journal of the Sanitary Engineering Division*, v. 88, no. SA4, p. 1-46.
- Elmore, H.L., and West, W.F., 1961, Effect of water temperature on stream reaeration: American Society of Civil Engineers, *Journal of the Sanitary Engineering Division*, v. 87, no. SA6, p. 59-71.
- Fischer, H.B., 1966, A note on the one-dimensional dispersion model: *Air and Water Pollution International Journal*, v. 10, p. 443-452.
- 1968, Dispersion predictions in natural streams: American Society of Civil Engineers, *Journal of the Sanitary Engineering Division*, v. 94, no. SA5, p. 927-943.
- Fischer, H.B., List, E.J., Koh, R.C.Y., Imberger, J., Brooks, N.H., 1979, *Mixing in inland and coastal waters*: New York, Academic Press, 483 p.
- Hubbard, E.F., Kilpatrick, F.A., Martens, L.A., Wilson, J.F., Jr., 1982, Measurement of time of travel and dispersion in streams by dye tracing: U.S. Geological Survey *Techniques of Water Resources Investigations Book 3, Chap. A9*, 44 p.
- International Souris-Red Rivers Engineering Board, 1980, Impacts on Canada of operation of the Burlington Project, Souris River, North Dakota: Report to the International Joint Commission, March 1980, 77 p.

- Isaacs, W.P., and Gaudy, A.F., 1968, Atmospheric oxygenation in a simulated stream: American Society of Civil Engineers, Journal of the Sanitary Engineering Division, v. 94, no. SA2, p. 319-344.
- Kilpatrick, F.A., Rathbun, R.E., Yotsukura, N., and Parker, G.W., 1987, Determination of stream reaeration coefficients by use of tracers: U.S. Geological Survey Open-File Report 87-245, 84 p.
- Krenkel, P.A., and Orlob, G.T., 1963, Turbulent diffusion and the reaeration coefficient: American Society of Civil Engineers Transactions, v. 128, Part III, Paper no. 3491, p. 293-334.
- Langbein, W.B., and Durum, W.H., 1967, The aeration capacity of streams: U.S. Geological Survey Circular 542, 6 p.
- Lau, Y.L., 1972, Prediction equations of reaeration in open-channel flow: American Society of Civil Engineers, Journal of the Sanitary Engineering Division, v. 98, no. SA6, p. 1063-1068.
- Negulescu, M., and Rojanski, V., 1969, Recent research to determine reaeration coefficient: Water Research, v. 3, no. 3, p. 189-202.
- North Dakota State Department of Health, 1977, Standards of water quality for State of North Dakota: Regulation 61-28-02, 20 p.
- 1979, North Dakota statewide 208 water quality management plan: 106 p.
- O'Connor, D.J., and Dobbins, W.E., 1958, Mechanism of reaeration in natural streams: American Society of Civil Engineers Transactions, v. 123, Paper no. 2934, p. 641-684.
- Owens, M., Edwards, R.W., and Gibbs, J.W., 1964, Some reaeration studies in streams: International Journal of Air and Water Pollution, v. 8, no. 819, p. 469-486.
- Padden T.J. and Gloyna, E.F., 1971, Simulation of stream processes in a model river: Austin, Texas, University of Texas Report no. EHE-70-23, CRWR-72.
- Parkhurst, J.D., and Pomeroy, R.D., 1972, Oxygen absorption in streams: American Society of Civil Engineers, Journal of the Sanitary Engineering Division, v. 98, no. SA1, p. 101-124.
- Rathbun, R.E., 1977, Reaeration coefficients of streams--state-of-the-art: American Society of Civil Engineers, Journal of the Hydraulics Division, v. 103, no. HY4, p. 409-424.
- 1979, Estimating the gas and dye quantities for modified tracer technique measurements of stream reaeration coefficients: U.S. Geological Survey Water-Resources Investigations 79-27, 42 p.

- Rathbun, R.E., Shultz, D.J., Stephens, D.W., 1975, Preliminary experiments with a modified tracer technique for measuring stream reaeration coefficients: U.S. Geological Survey Open-File Report 75-256, 36 p.
- Rathbun, R.E., Stephens, D.W., Shultz, D.J., and Tai, D.Y., 1978, Laboratory studies of gas tracer for reaeration: American Society of Civil Engineers, Journal of the Environmental Engineering Division, v. 104, no. EE2, p. 215-229.
- Regan, R.S., and Schaffranek, R.W., 1985, A computer program for analyzing channel geometry: U.S. Geological Survey Water-Resources Investigations Report 85-4335, 49 p.
- Swinnerton, J.W., and Linnenbom, J.V., 1967, Determination of the C<sub>1</sub> to C<sub>4</sub> hydrocarbons in sea water by gas chromatography: Journal of Gas Chromatography, v. 5, p. 570-573.
- Thackston, E.L., and Krenkel, P.A., 1969, Reaeration prediction in natural streams: American Society of Civil Engineers, Journal of the Sanitary Engineering Division, v. 95, no. SA1, p. 65-94.



Supplement 1.—Perspective plots of cross sections--Continued.



CROSS SECTIONS 54-56  
VIEWING ANGLE IS 75°

EXPLANATION

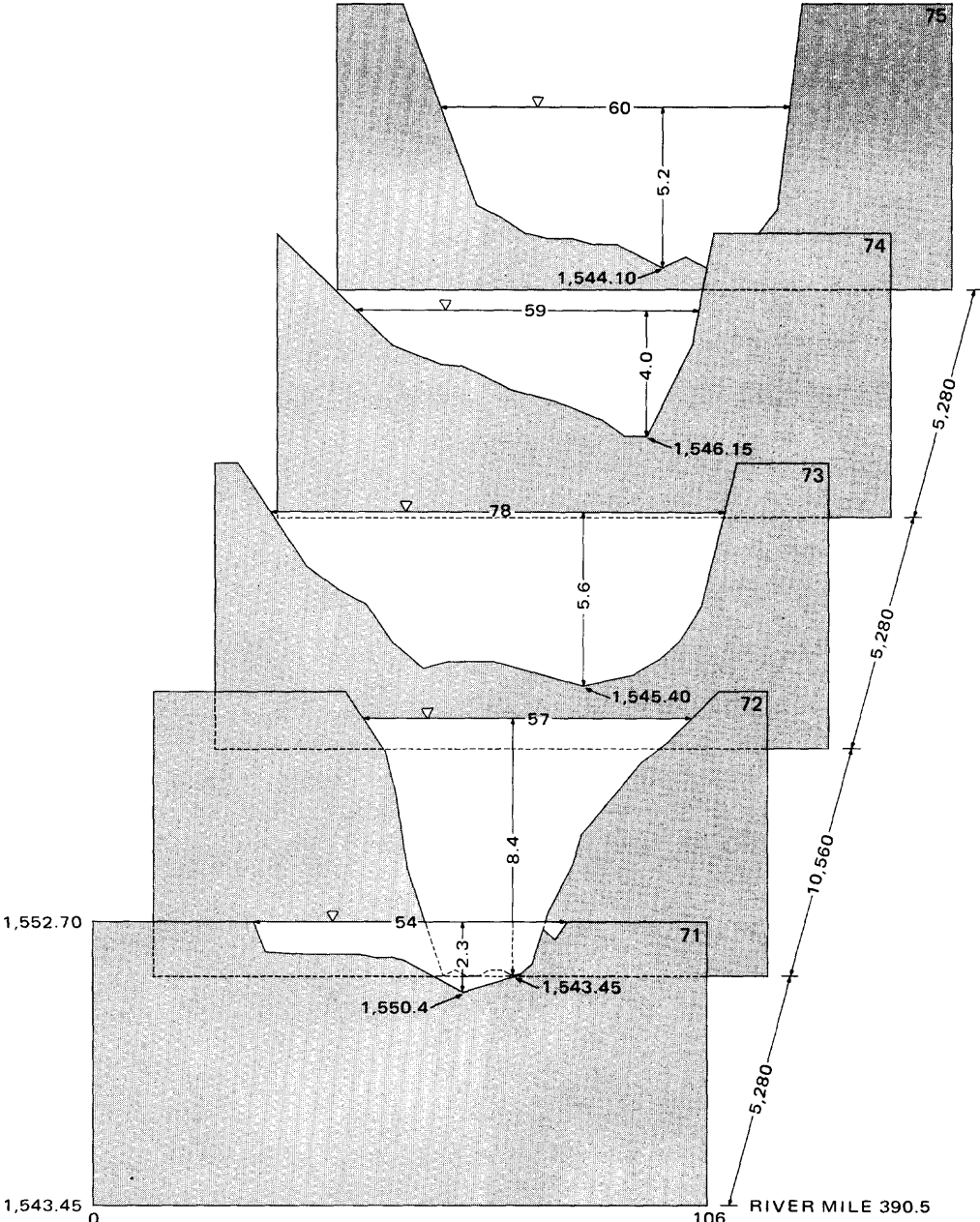
1,556.00 ELEVATION, IN FEET ABOVE SEA LEVEL

▽ WATER SURFACE

ALL DIMENSIONS ARE IN FEET UNLESS OTHERWISE INDICATED

Figure 15.—Six cross sections in the Foxholm test reach, September 9, 1983--Continued.

Supplement 1.—Perspective plots of cross sections--Continued.



CROSS SECTIONS 71-75  
VIEWING ANGLE IS 75°

EXPLANATION

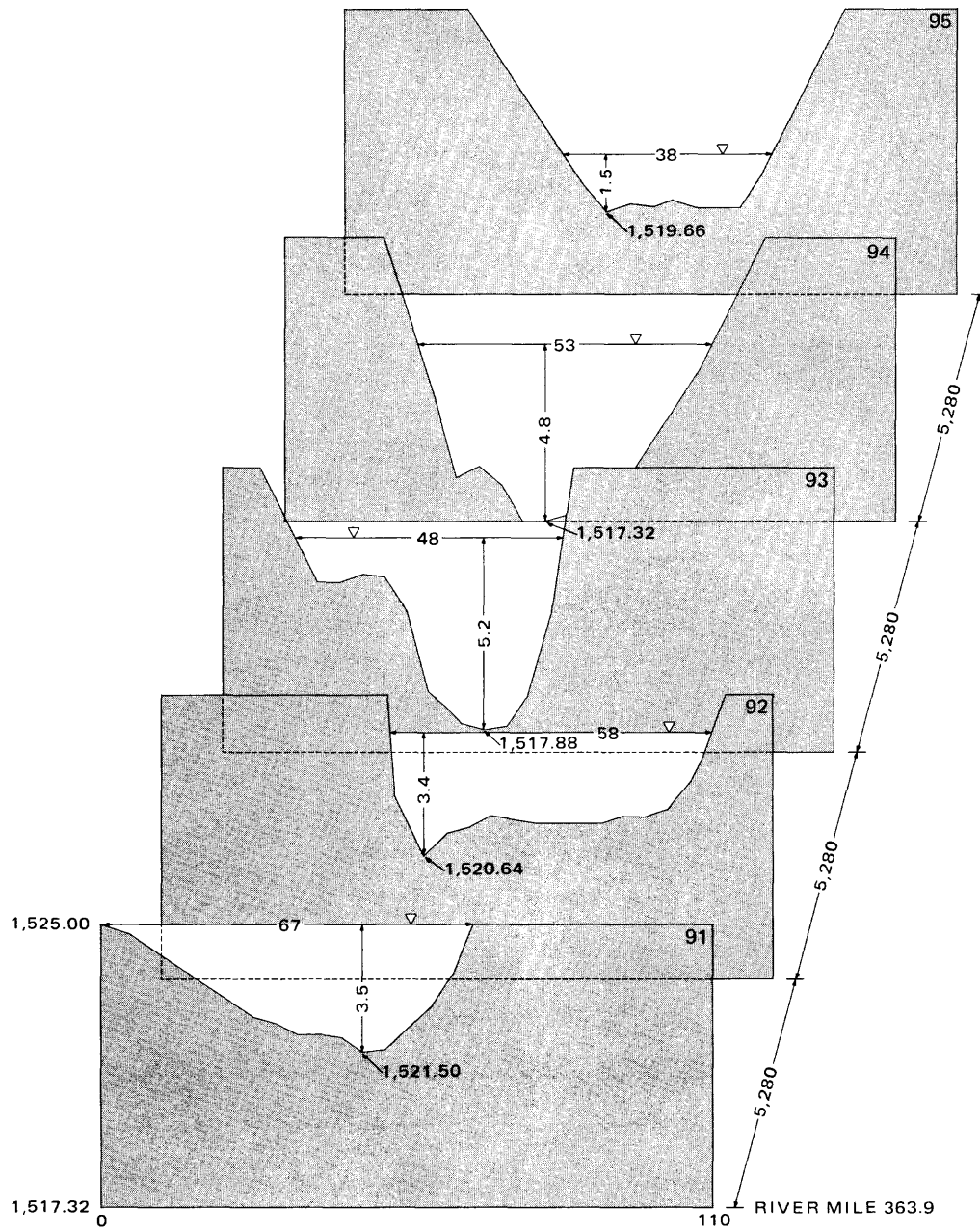
1,543.45 ELEVATION, IN FEET ABOVE SEA LEVEL

▽ WATER SURFACE

ALL DIMENSIONS ARE IN FEET UNLESS OTHERWISE INDICATED

Figure 16.—Five cross sections in the Minot test reach, September 21, 1983.

Supplement 1.—Perspective plots of cross sections--Continued.



CROSS SECTIONS 91-95  
VIEWING ANGLE IS 75°

EXPLANATION

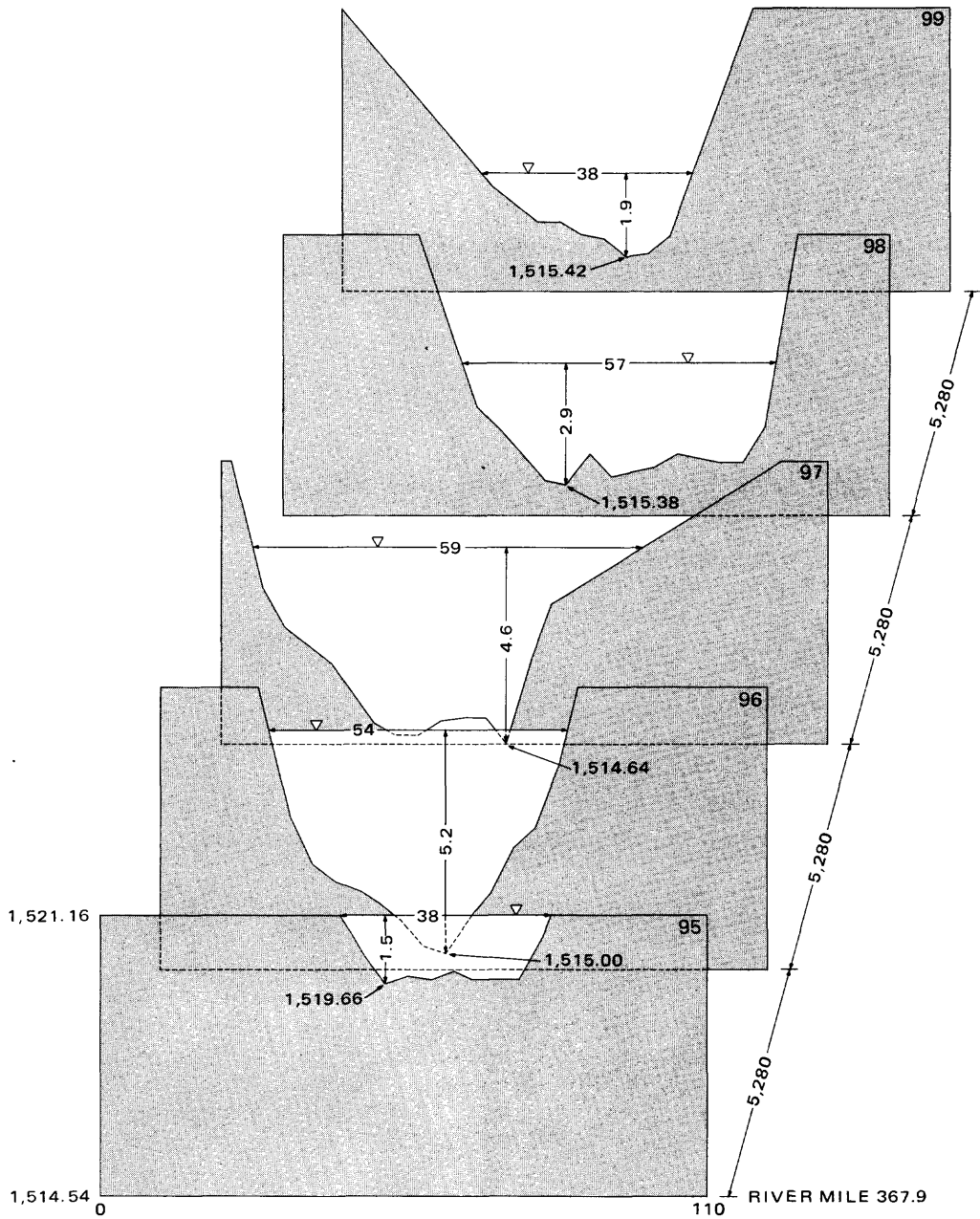
1,517.32 ELEVATION, IN FEET ABOVE SEA LEVEL

▽ WATER SURFACE

ALL DIMENSIONS ARE IN FEET UNLESS  
OTHERWISE INDICATED

Figure 17.—Nine cross sections in the Logan test reach, September 22, 1983.

Supplement 1.—Perspective plots of cross sections--Continued.



CROSS SECTIONS 95-99  
VIEWING ANGLE IS 75°

EXPLANATION

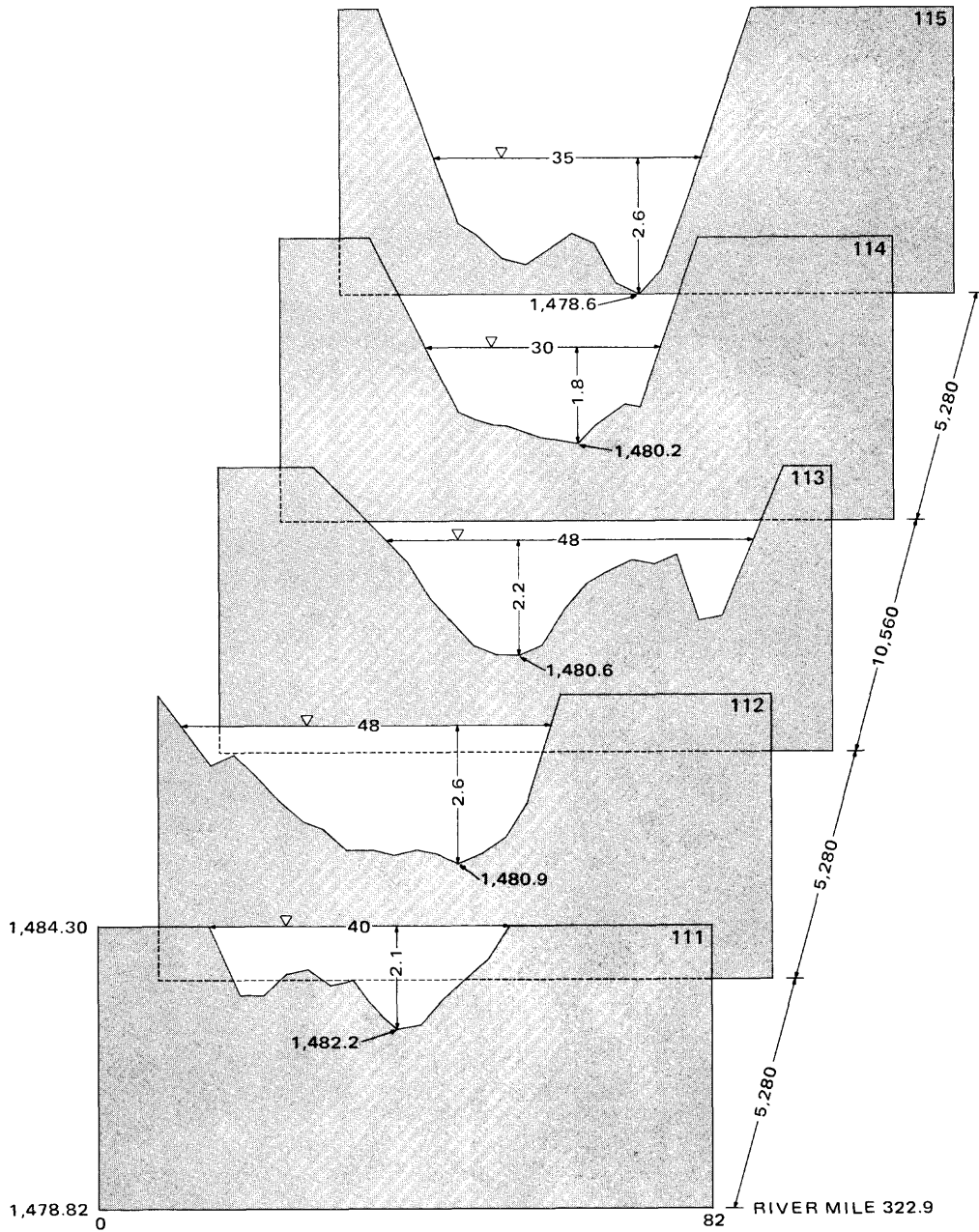
1,514.54 ELEVATION, IN FEET ABOVE SEA LEVEL

▽ WATER SURFACE

ALL DIMENSIONS ARE IN FEET UNLESS  
OTHERWISE INDICATED

Figure 17.—Nine cross sections in the Logan test reach, September 22, 1983--Continued.

Supplement 1.—Perspective plots of cross sections--Continued.



CROSS SECTIONS 111-115  
VIEWING ANGLE IS 75°

EXPLANATION

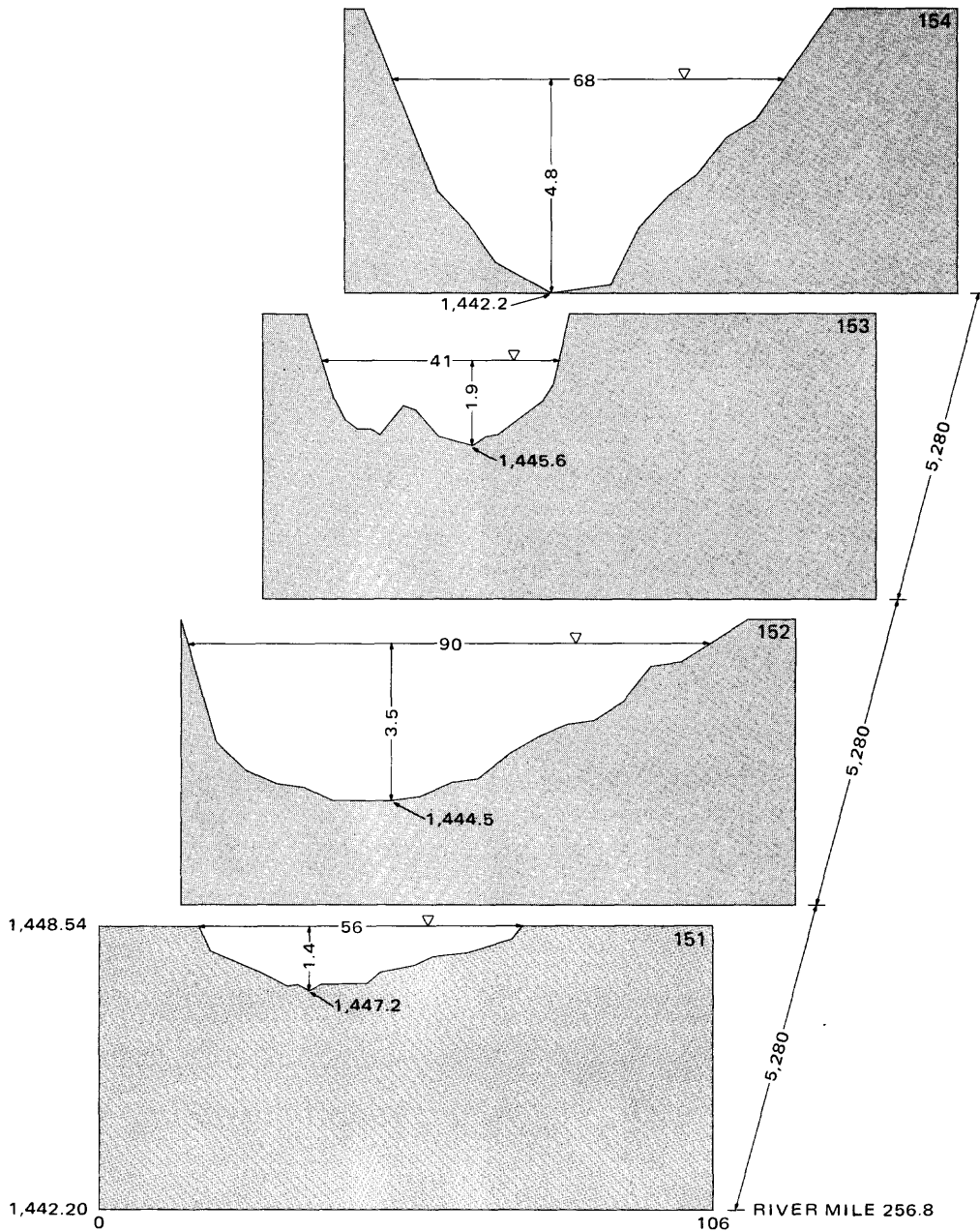
1,478.82 ELEVATION, IN FEET ABOVE SEA LEVEL

▽ WATER SURFACE

ALL DIMENSIONS ARE IN FEET UNLESS OTHERWISE INDICATED

Figure 18.—Five cross sections in the Velva test reach, September 28, 1983.

Supplement 1.—Perspective plots of cross sections--Continued.



CROSS SECTIONS 151-154  
VIEWING ANGLE IS 75°

EXPLANATION

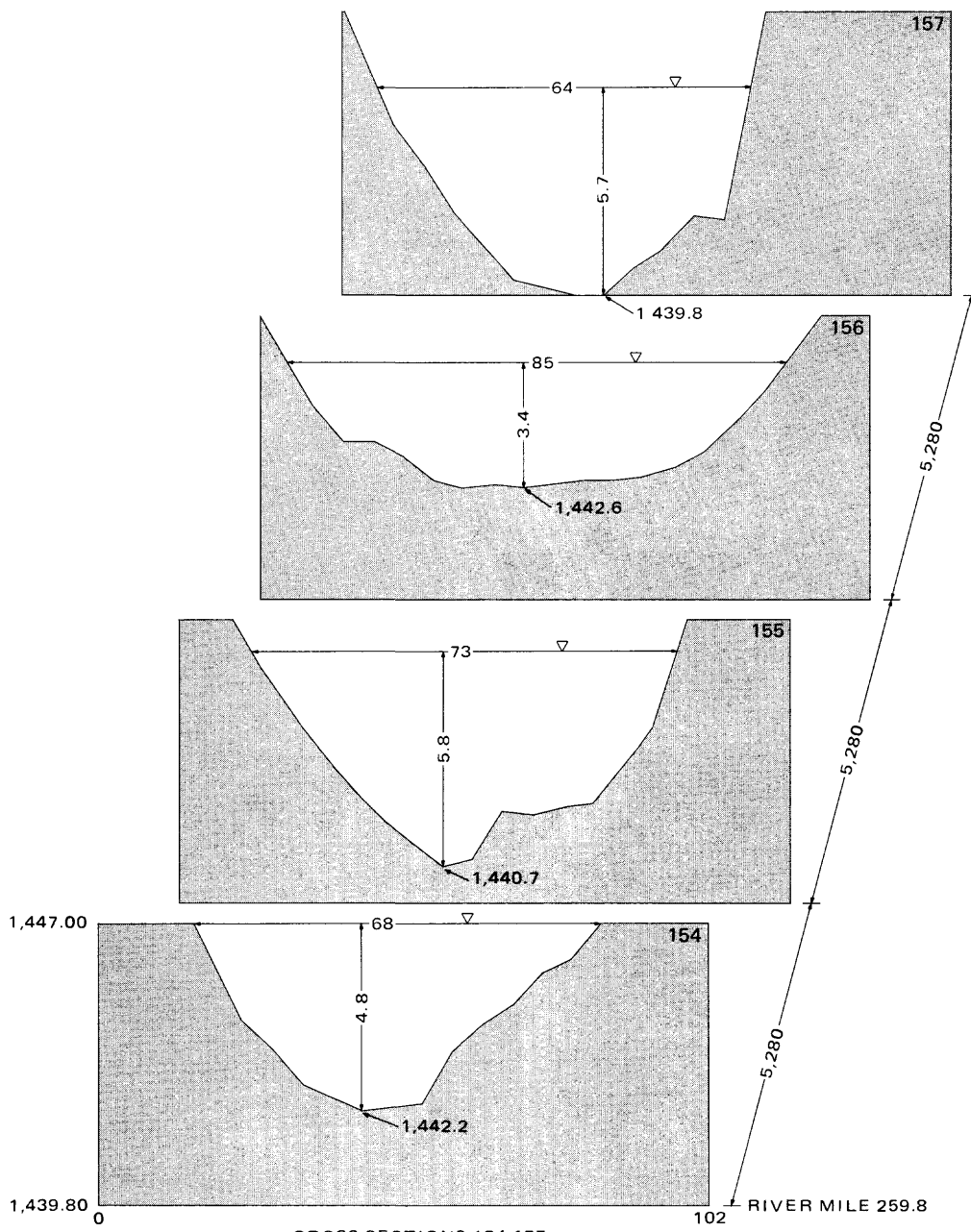
1,442.20 ELEVATION, IN FEET ABOVE SEA LEVEL

▽ WATER SURFACE

ALL DIMENSIONS ARE IN FEET UNLESS OTHERWISE INDICATED

Figure 19.—Seven cross sections in the Towner test reach, September 27, 1983.

Supplement 1.—Perspective plots of cross sections--Continued.



CROSS SECTIONS 154-157  
VIEWING ANGLE IS 75°

EXPLANATION

1,439.80 ELEVATION, IN FEET ABOVE SEA LEVEL

▽ WATER SURFACE

ALL DIMENSIONS ARE IN FEET UNLESS OTHERWISE INDICATED

Figure 19.—Seven cross sections in the Towner test reach, September 27, 1983--Continued.

Supplement 2.—Measured dye concentrations as a function of traveltime.

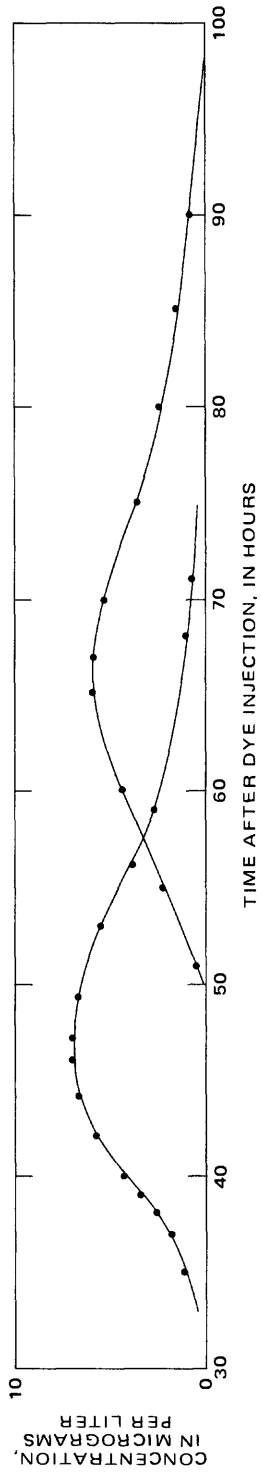


Figure 20.—Measured dye concentrations as a function of traveltime, Foxholm test reach, September 6-11, 1983.

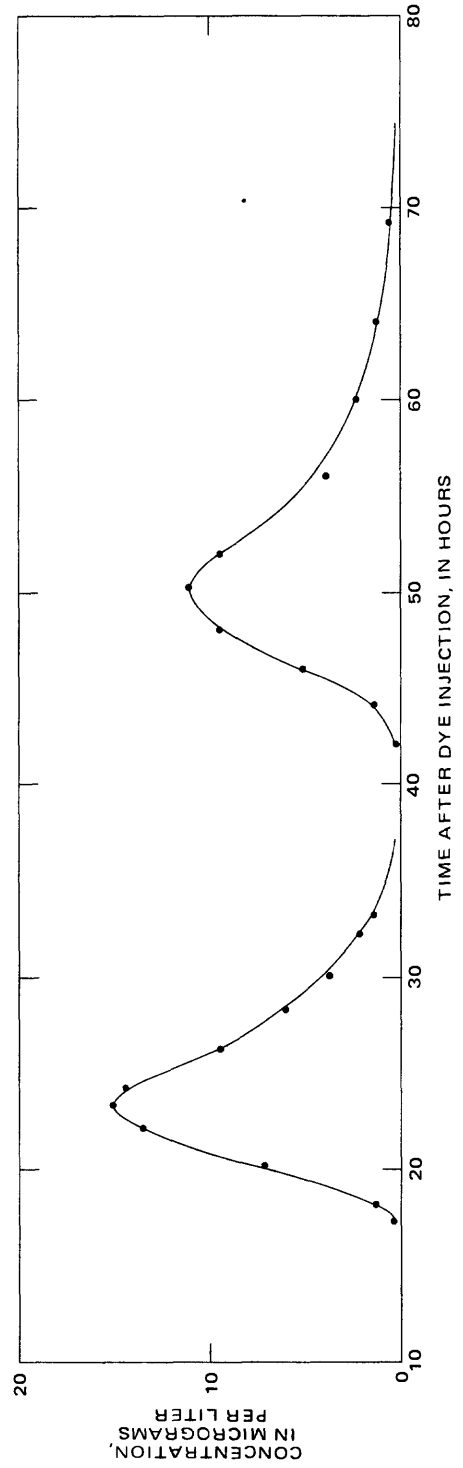


Figure 21.—Measured dye concentrations as a function of traveltime, Minnot test reach, September 7-10, 1983.

Supplement 2.—Measured dye concentrations as a function of traveltime--Continued.

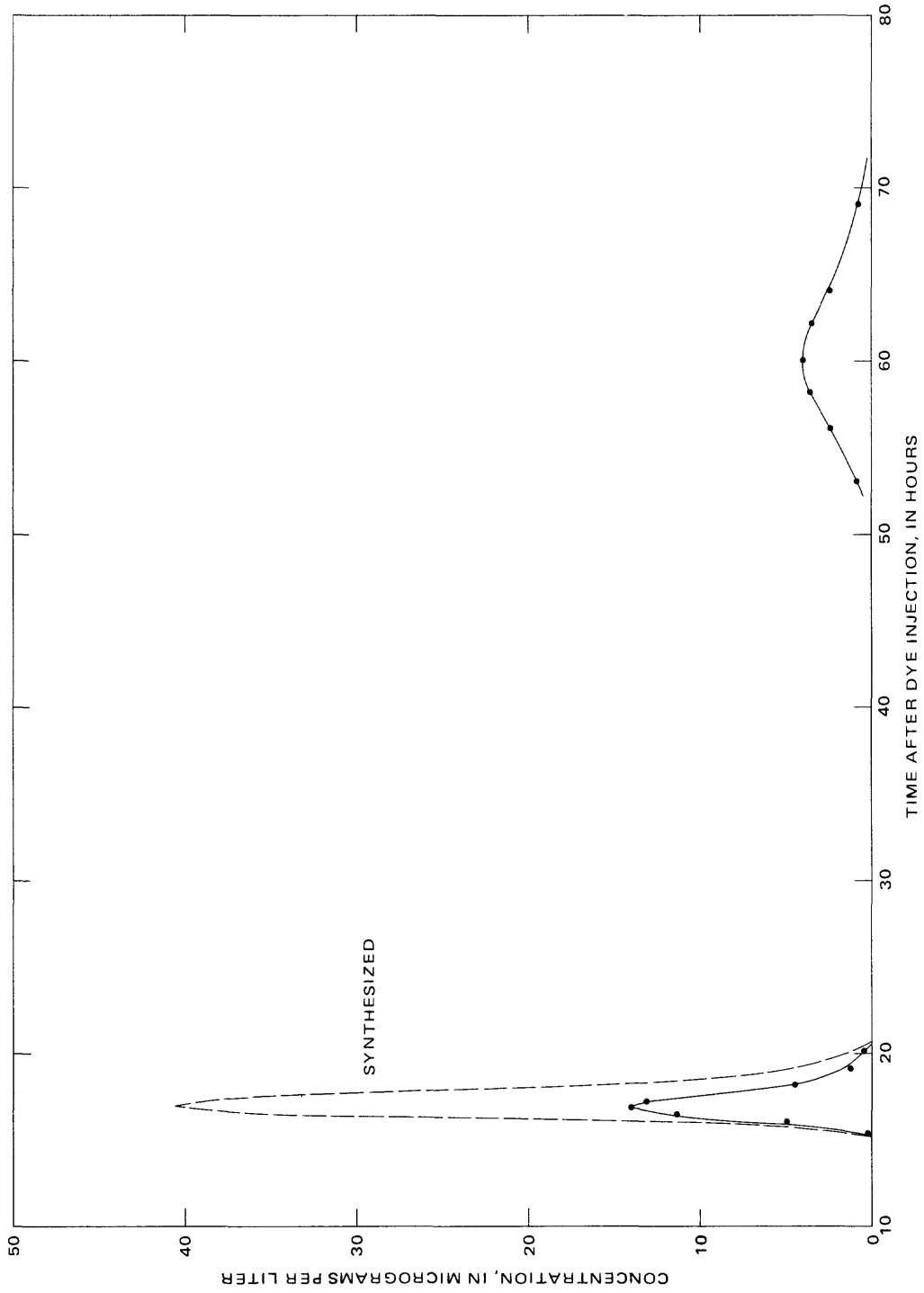


Figure 22.—Measured dye concentrations as a function of traveltime, Logan test reach, September 14-17, 1983.

Supplement 2.—Measured dye concentrations as a function of traveltime--Continued.

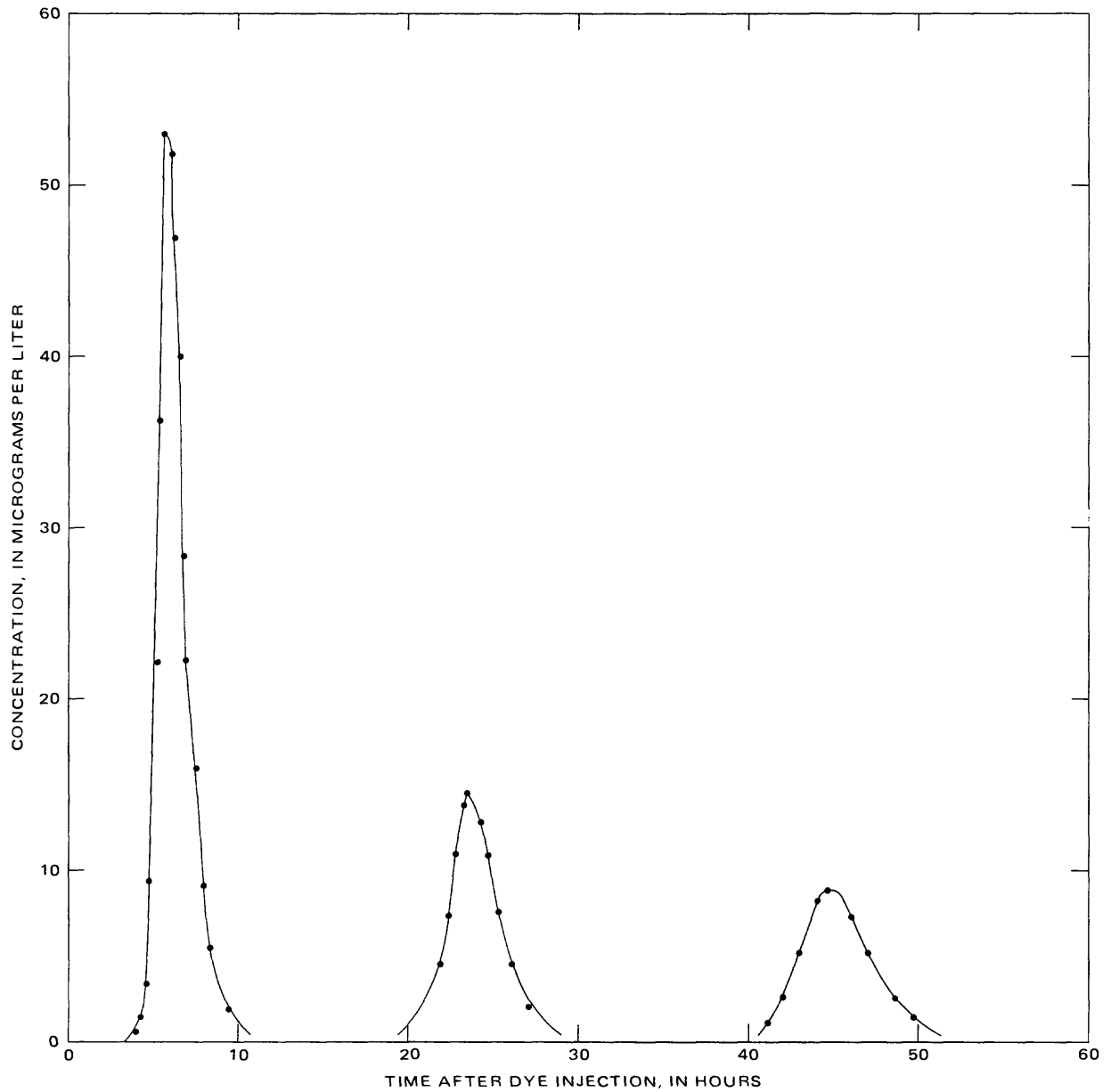


Figure 23.—Measured dye concentrations as a function of traveltime, Velva test reach, September 14-16, 1983.

Supplement 2.—Measured dye concentrations as a function of traveltime--Continued.

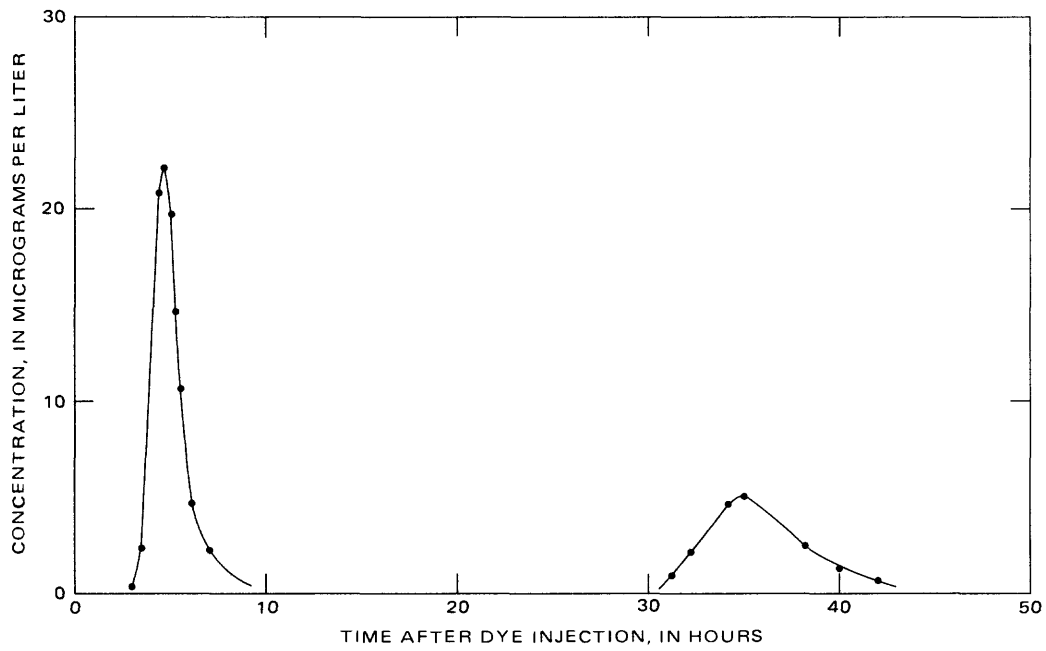


Figure 24.—Measured dye concentrations as a function of traveltime, Towner test reach, September 27-29, 1983.

Supplement 3.—Traveltime as a function of distance relations.

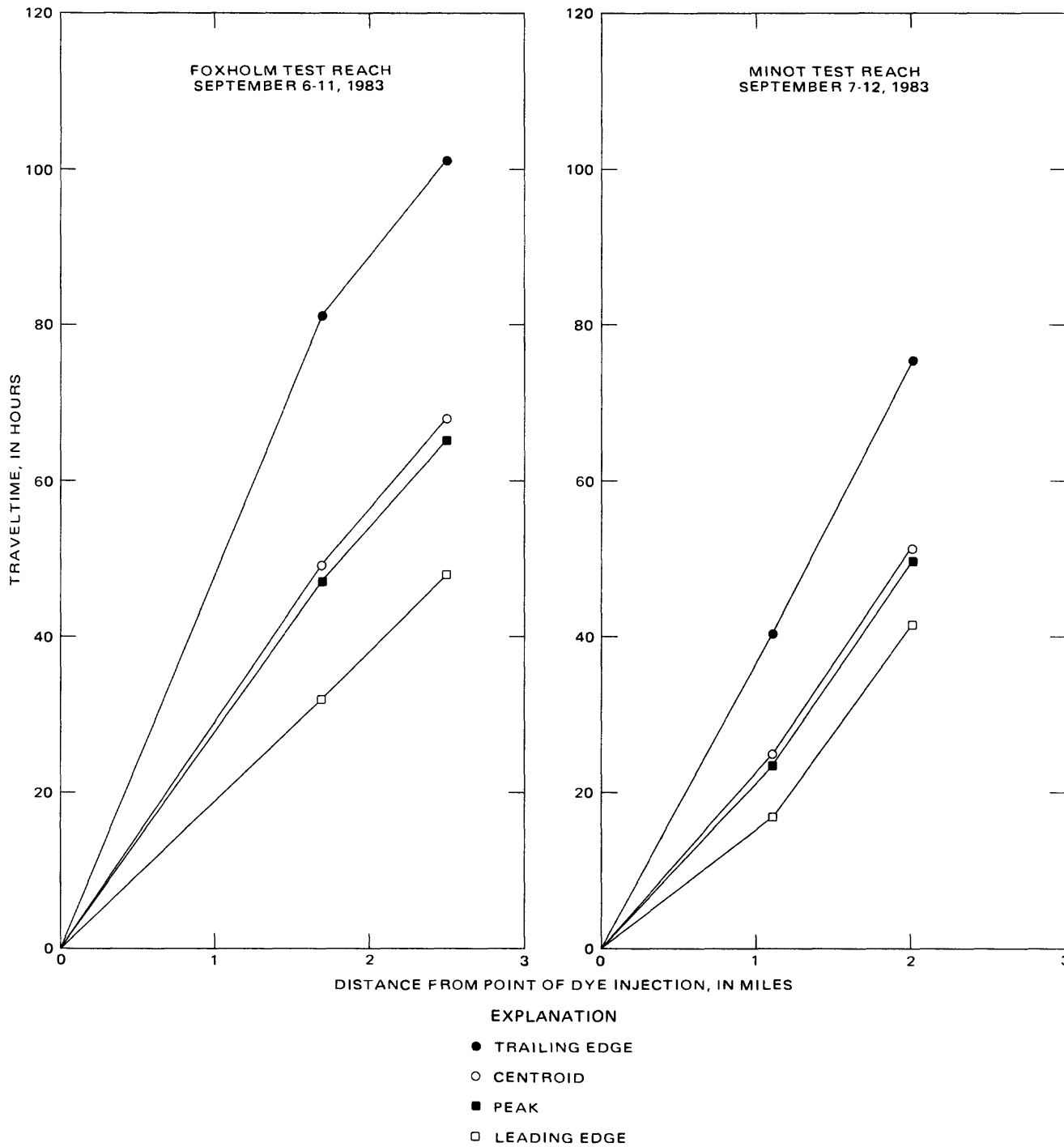


Figure 25.—Traveltime as a function of distance relations for the Foxholm and Minot test reaches.

Supplement 3.—Traveltime as a function of distance relations--Continued.

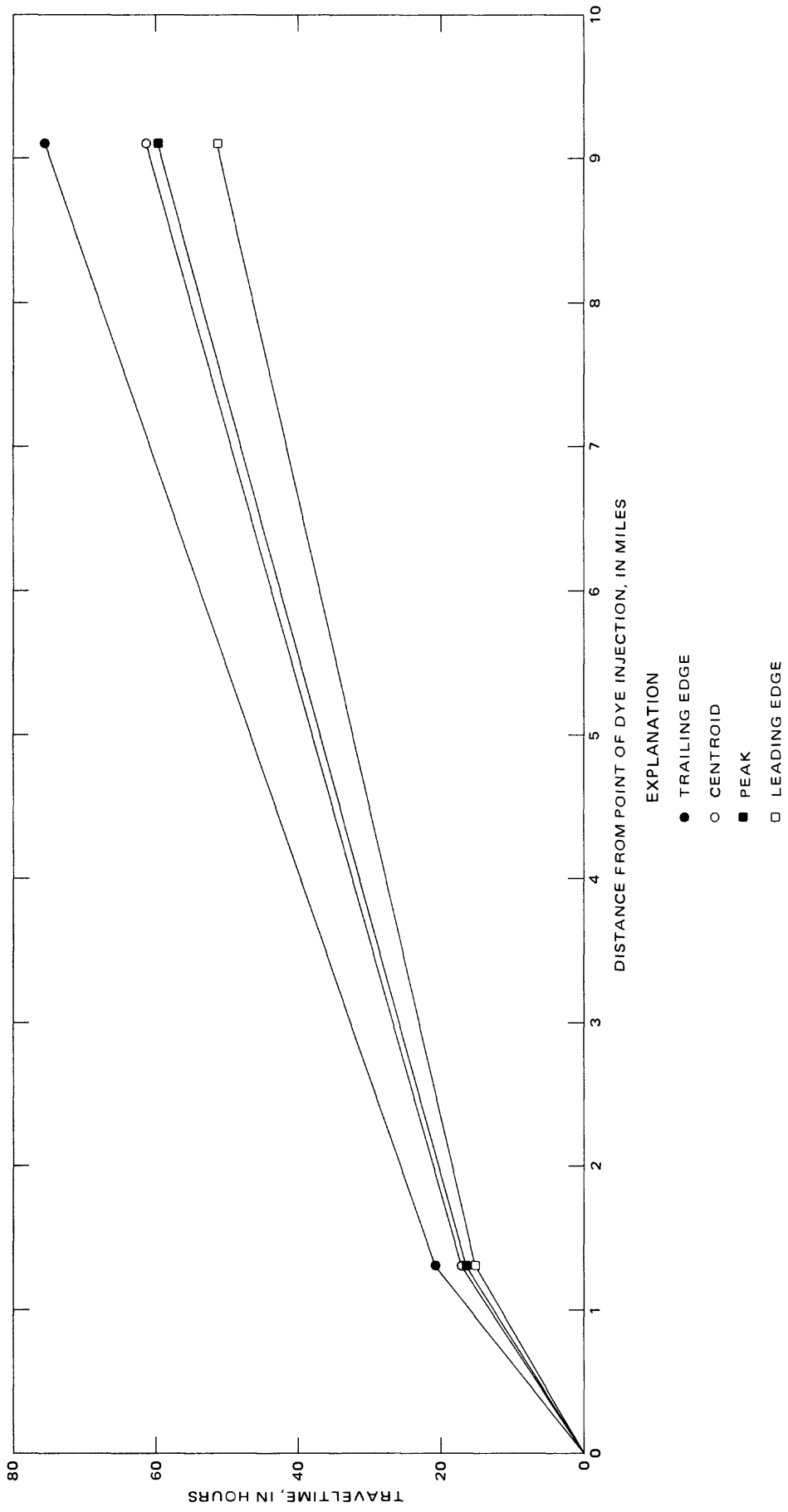


Figure 26.—Traveltime as a function of distance relations for the Logan test reach, September 14-17, 1983.

Supplement 3.—Traveltime as a function of distance relations--Continued.

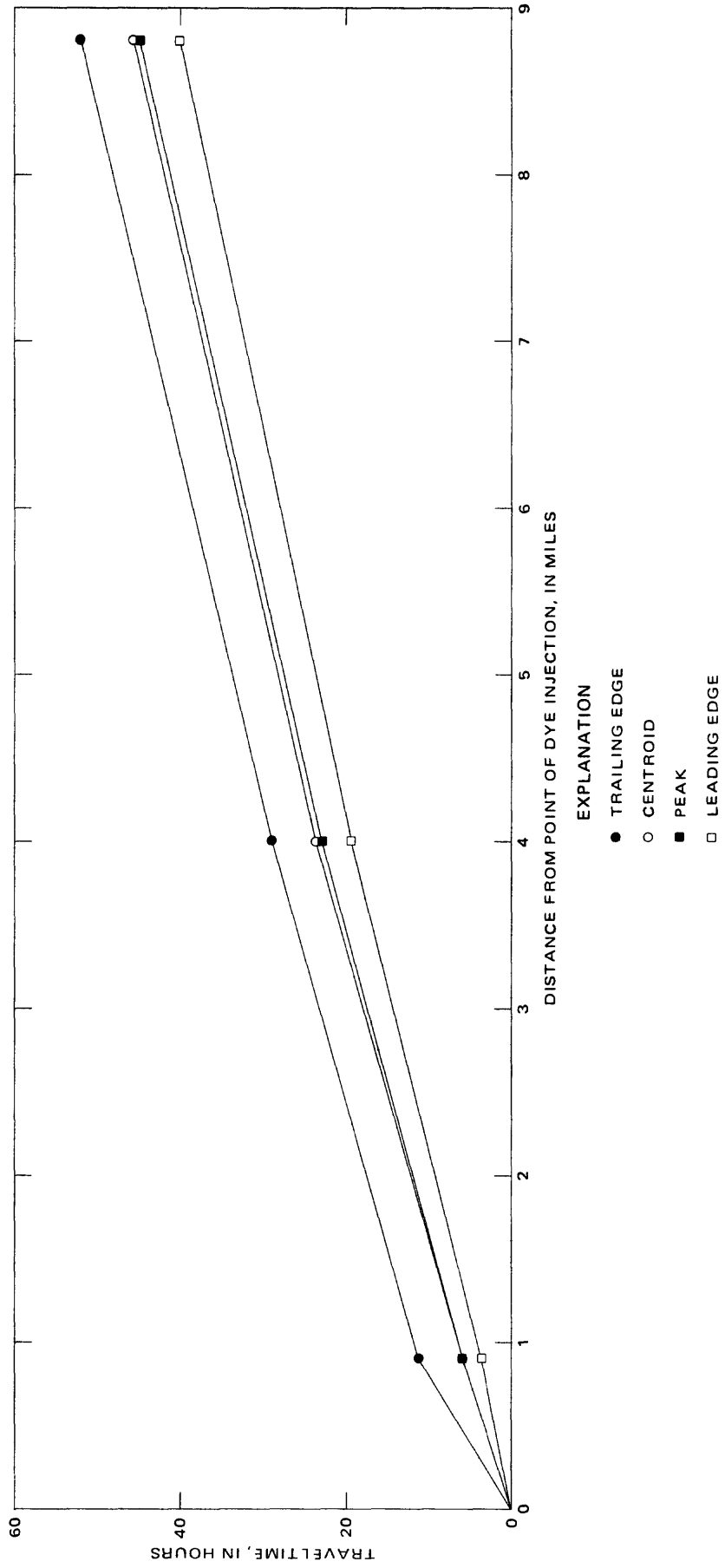


Figure 27.—Traveltime as a function of distance relations for the Velva test reach, September 14-16, 1983.

Supplement 3.—Traveltime as a function of distance relations--Continued.

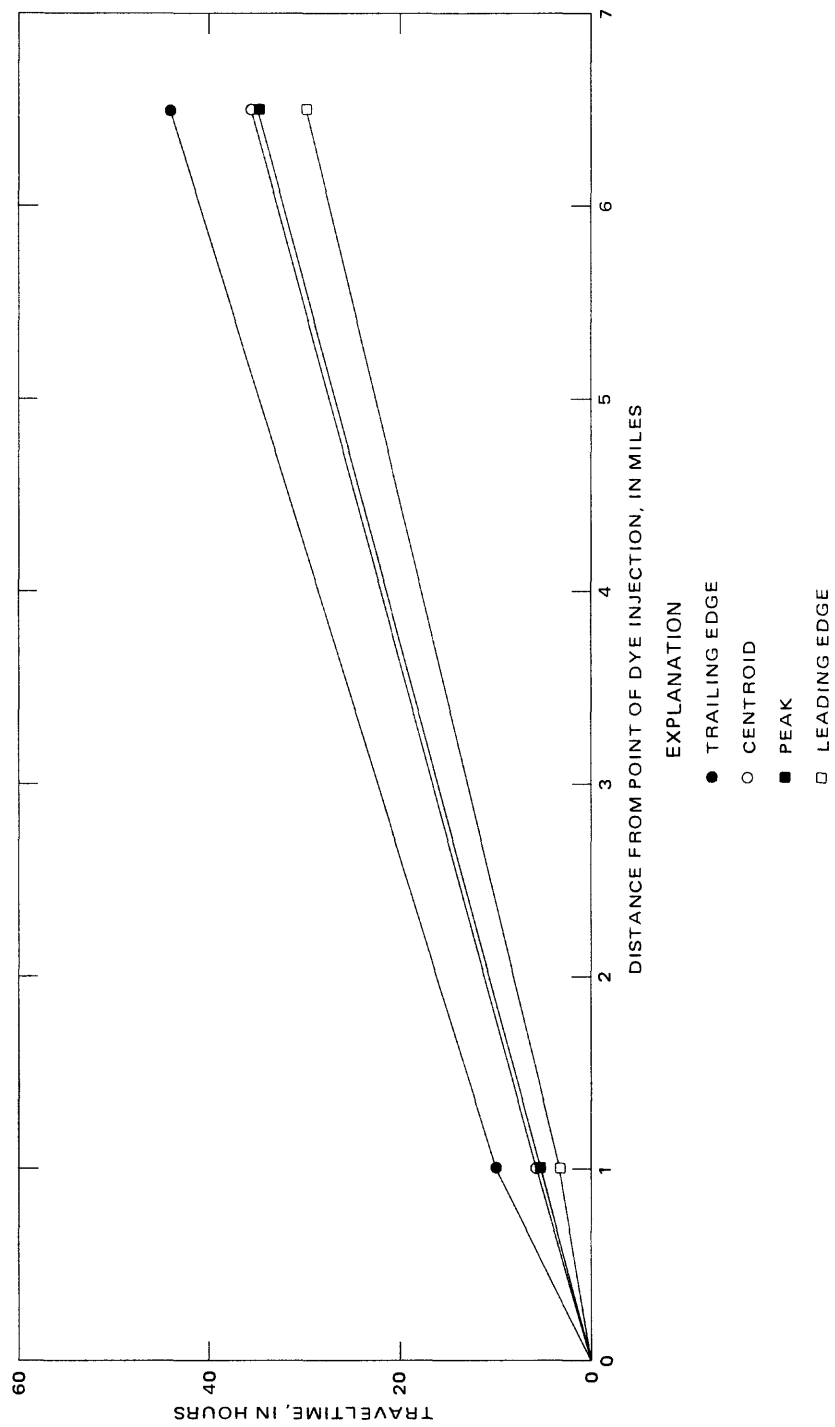


Figure 28.—Traveltime as a function of distance relations for the Towner test reach, September 27-29, 1983.

Supplement 4.--Reconstruction and calculation of area under concentration-time curve for the Logan test reach using total-recovery equation.

To determine the area under the concentration-time curve for the first sampling cross section in the Logan test reach, the total-recovery equation of Hubbard and others (1982) was used. The total-recovery equation indicates, if a tracer is conservative, that the total volume injected upstream will be recovered downstream by:

$$Ac = \frac{Vol C_s}{Q}$$

where  $Ac$  = concentration-time area after complete mixing, in micrograms-hour per liter;

$Vol$  = volume of dye injected, in liters;

$C_s$  = dye concentration, in micrograms per liter; and

$Q$  = discharge at the point of sampling, in cubic feet per second.

For the first Logan sampling cross section,

$$Ac = \frac{2.8 (1.19)(5 \times 10^7)}{20 (101,952)} = 81.7$$

An 85-percent dye recovery was assumed, so the  $Ac$  would be decreased to 69.45. To synthesize an area under the curve to represent 85-percent recovery, each measured concentration-time coordinate was multiplied by a factor of  $69.45/24.05 = 2.89$ . As a result of this synthesis, the measured dye peak for the Logan test reach was calculated by multiplying the measured dye peak (14  $\mu\text{g/L}$ ) by the synthesis factor (2.89) to obtain 40.5; the conservative dye peak would be 48  $\mu\text{g/L}$  ( $40.5 \times 100/85$ ).

Supplement 5.—Measured-, conservative-, and unit-peak dye concentrations as a function of traveltime.

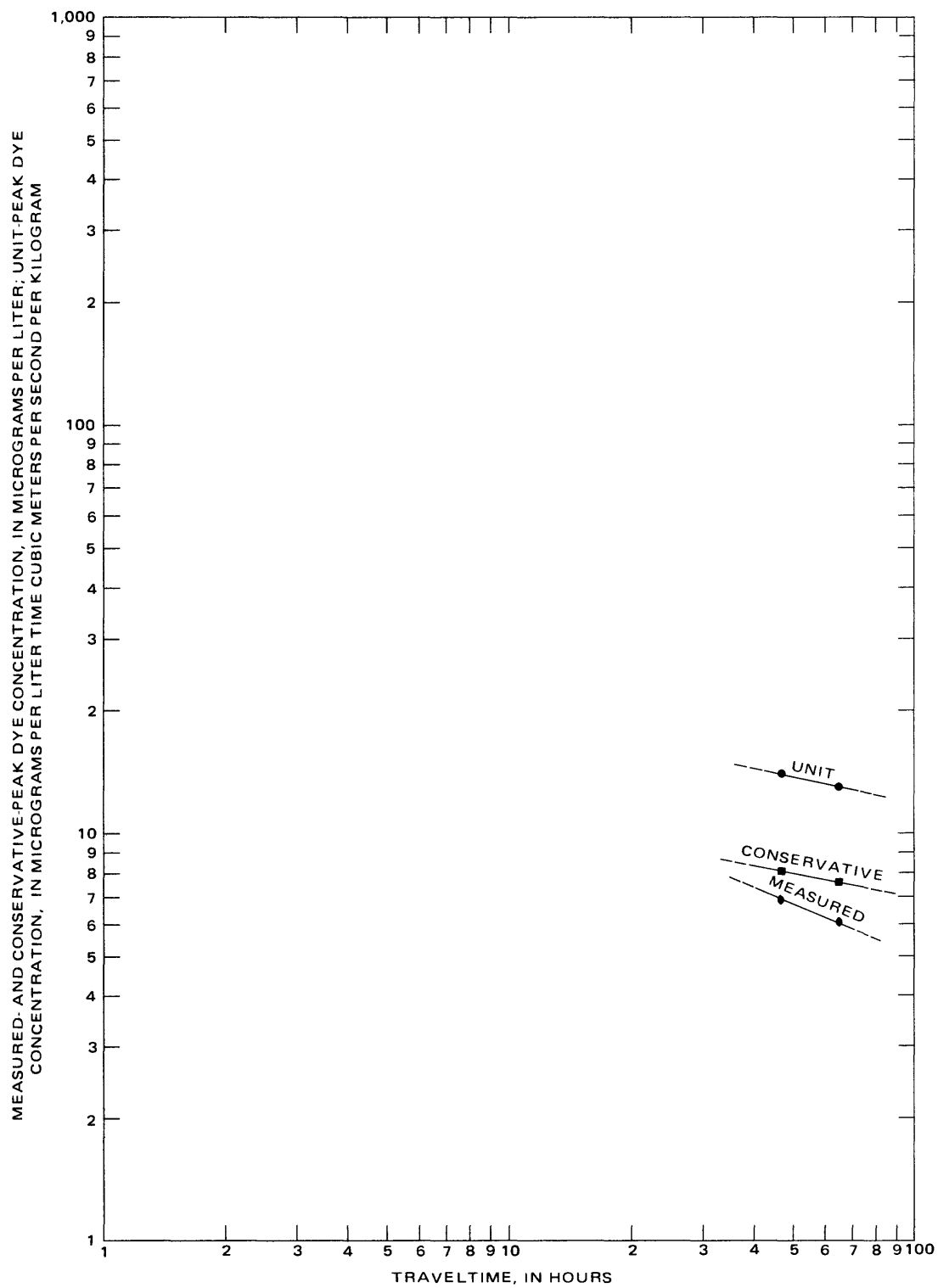


Figure 29.—Measured-, conservative-, and unit-peak dye concentrations as a function of traveltime for the Foxholm test reach.

Supplement 5.—Measured-, conservative-, and unit-peak dye concentrations as a function of traveltime--Continued.

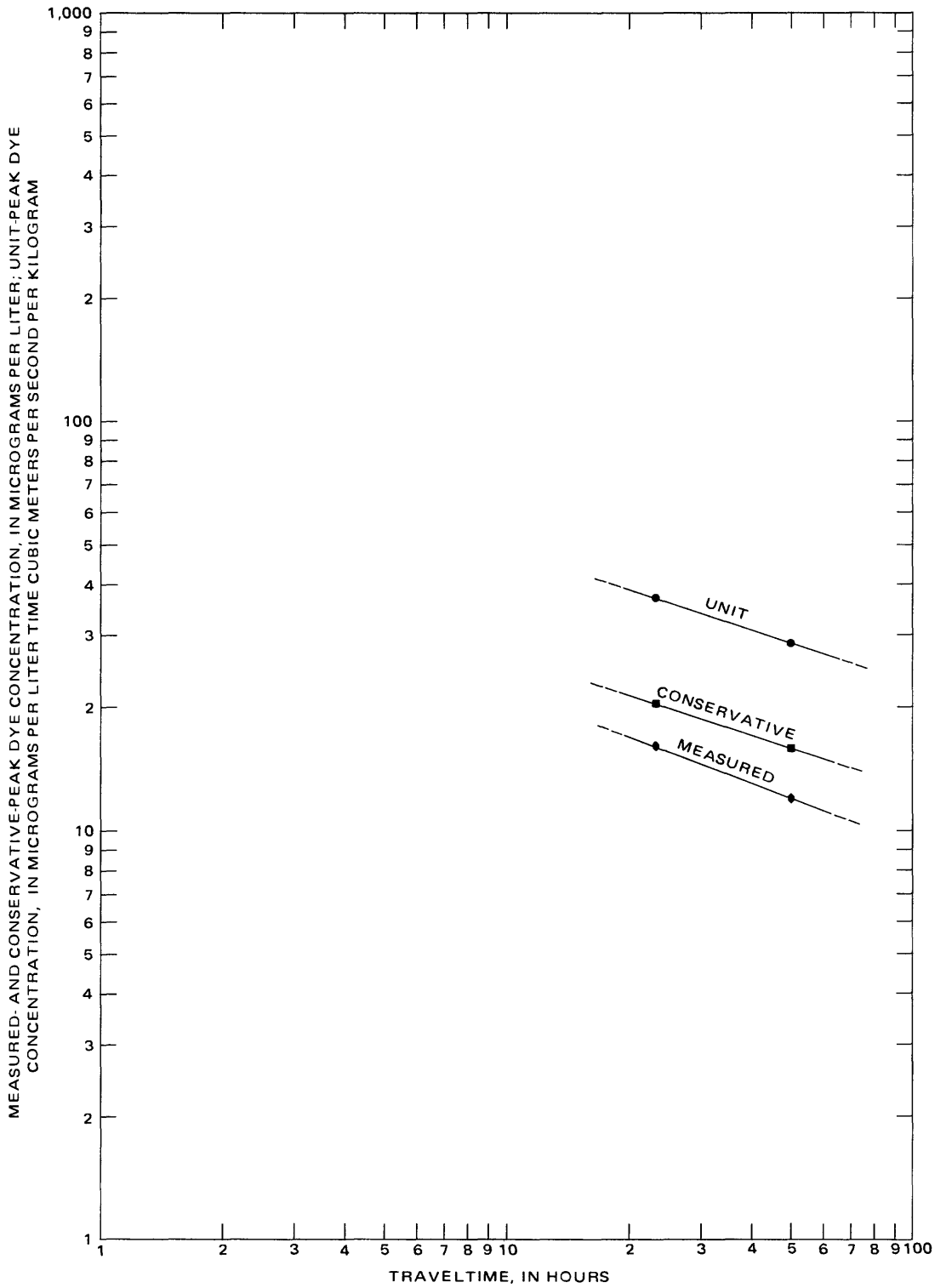


Figure 30.—Measured-, conservative-, and unit-peak dye concentrations as a function of traveltime for the Minot test reach.

Supplement 5.—Measured-, conservative-, and unit-peak dye concentrations as a function of traveltime—Continued.

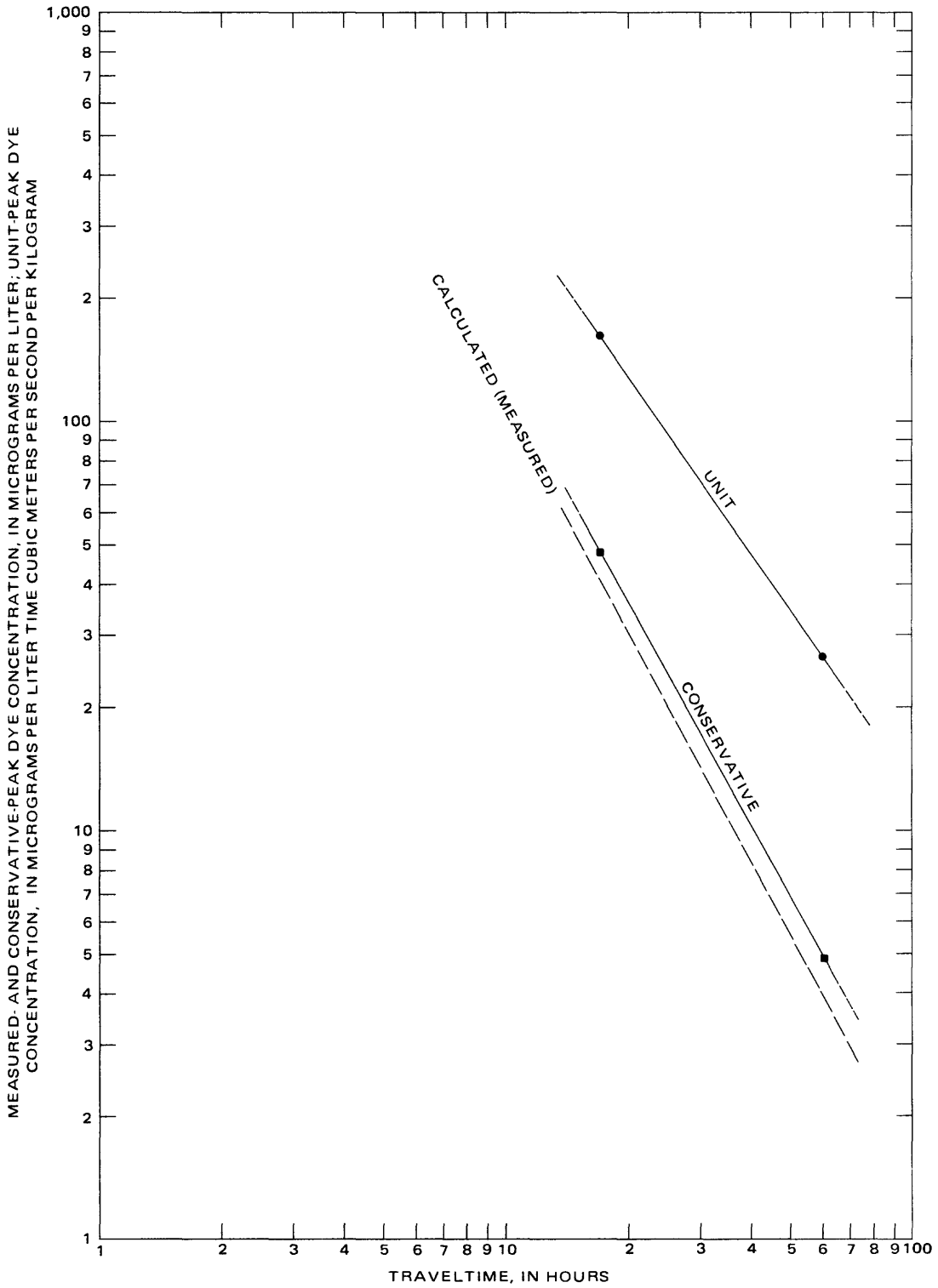


Figure 31.—Measured-, conservative-, and unit-peak dye concentrations as a function of traveltime for the Logan test reach.

Supplement 5.—Measured-, conservative-, and unit-peak dye concentrations as a function of traveltime--Continued.

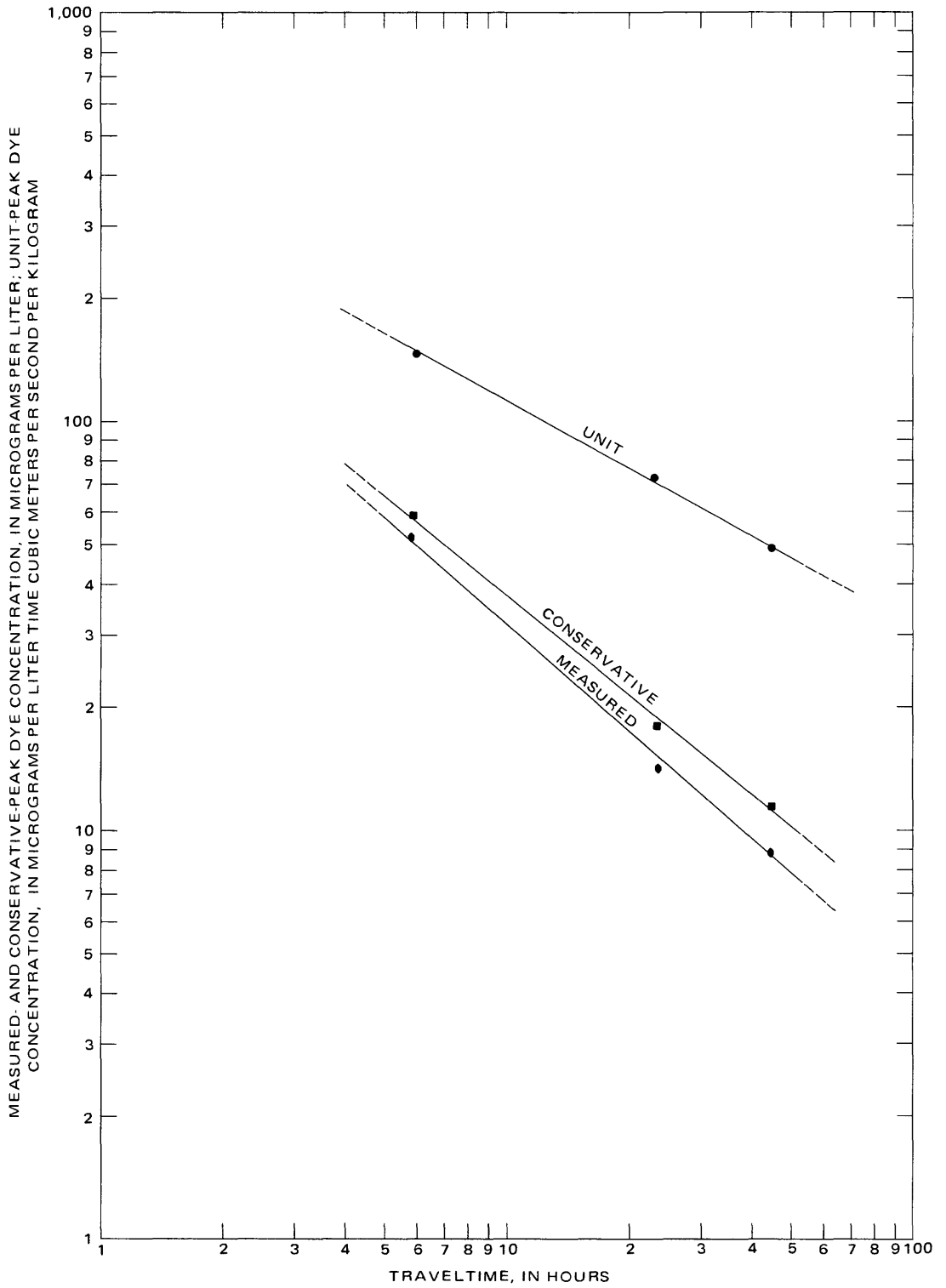


Figure 32.—Measured-, conservative-, and unit-peak dye concentrations as a function of traveltime for the Velva test reach.

Supplement 5.—Measured-, conservative-, and unit-peak dye concentrations as a function of traveltime--Continued.

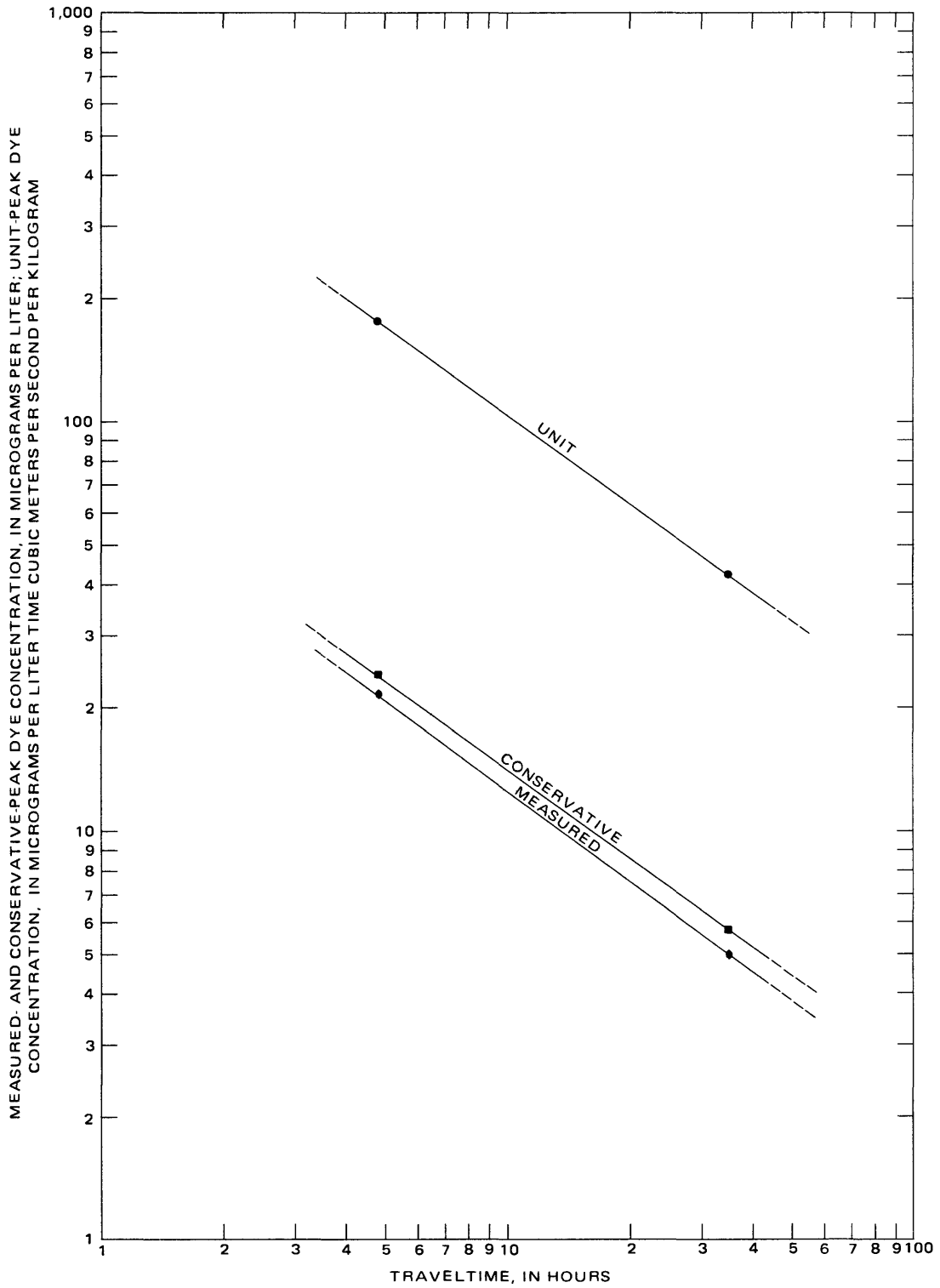


Figure 33.—Measured-, conservative-, and unit-peak dye concentrations as a function of traveltime for the Towner test reach.